



ROUTINE CORE ANALYSIS FINAL REPORT
of
MEGASCOLIDES-1ST
for
KAROON GAS AUSTRALIA LTD
by
ACS LABORATORIES PTY LTD



28th February, 2007

Karoon Gas Australia Ltd
Level 9
406 Collins Street
MELBOURNE VIC 3000

Attention: Lino Barro

FINAL REPORT: 0387-02
MEGASCOLIDES-1ST

CLIENT REFERENCE: Purchase Order No. 249
MATERIAL: 4" Diameter Whole Core
LOCALITY: PEP 162
WORK REQUIRED: Routine Core Analysis

Please direct technical inquiries regarding this work to the signatory below under whose supervision the work was conducted.

NICK COX
Operations Manager

ACS Laboratories Pty. Ltd. shall not be liable or responsible for any loss, cost, damages or expenses incurred by the client, or any other person or company, resulting from any information or interpretation given in this report. In no case shall ACS Laboratories Pty. Ltd. be responsible for consequential damages including, but not limited to, lost profits, damages for failure to meet deadlines and lost production arising from this report.

Head Office: 8 Cox Road, Windsor Qld 4030, Australia
☎: 61 7 3357 1133 Facsimile: 61 7 3357 1100
E-mail: info@acslabs.com.au

ACS Laboratories Pty Ltd
ABN: 81 008 273 005

CONTENTS

CHAPTERS

Page

1.	INTRODUCTION	1
2.	SUMMARY	3
3.	ROUTINE CORE ANALYSIS	
3.1	Test and Calculation Procedures	
3.1.1	Sample Drilling	7
3.1.2	Probe Permeability	7
3.1.3	Continuous Core Gamma	7
3.1.4	Core Slabbing	7
3.1.5	Dean-Stark Residual Fluid Saturation	8
3.1.6	Salt Extraction Analysis	8
3.1.7	Cleaning and Drying	8
3.1.8	Porosity	9
3.1.9	Permeability to Air	9
3.1.10	Apparent Grain Density	10
3.1.11	Core Photography	10
3.2	Test Results	
3.2.1	Ambient Test Results	12
3.2.2	Water Analysis	15
3.2.3	Core Log Plot	17
4.	ELECTRICAL PROPERTIES	
4.1	Test and Calculation Procedures	
4.1.1	Base Parameters at Overburden Pressure	19
4.1.2	Sample Saturation	19
4.1.3	Formation Resistivity Factor	19
4.1.4	Continuous Injection Resistivity Index	20
4.1.5	Cation Exchange Capacity	21
4.2	Test Results	23
5.	SAMPLE DISTRIBUTION AND STORAGE	26

CONTENTS (cont.)

APPENDICES

- I. FLUID PROPERTIES**
- II. EQUIPMENT SCHEMATICS**
- III. PETROLOGY**

CHAPTER 1

INTRODUCTION

1. INTRODUCTION

ACS personnel travelled to the Megascolides–1ST well site on 23 December 2006 to process core. The cored intervals (1881.00m to 1887.60m, and 1887.60m to 1892.60m) were cut into one metre lengths before processing. The split core barrel was removed and core was marked with orientation lines and depth markings. Twelve horizontal and three vertical core plugs were cut at depths selected by the well site geologist in Core #1. Samples were preserved for analysis. The core was then replaced into core barrels. Core #2 was not processed on the rig site. All core material was then driven to Melbourne and transported to ACS Laboratories' Brisbane facility, arriving at 10.00 pm on 25 December 2006.

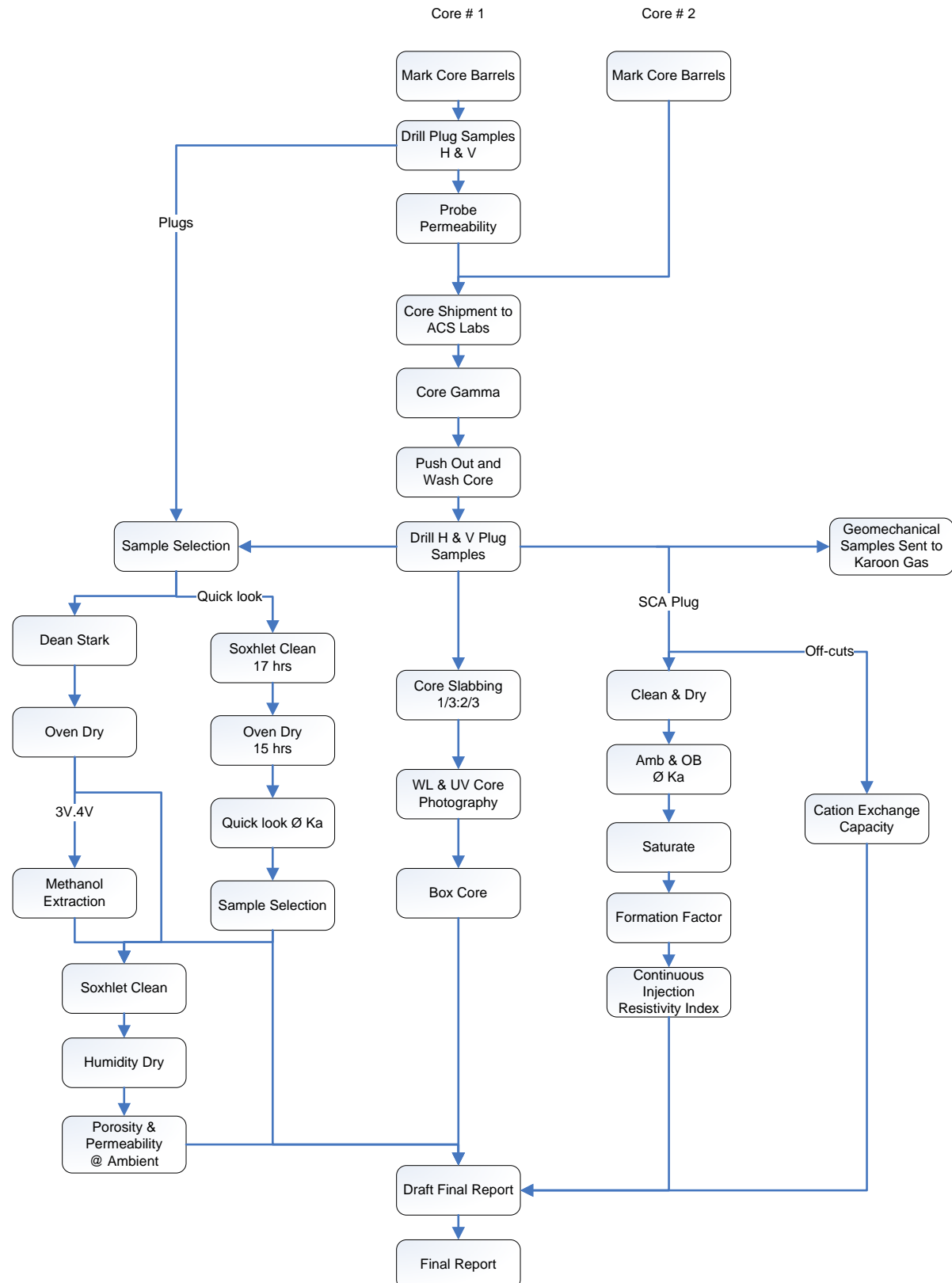
On receipt of core in the laboratory, routine core analysis was performed as per instructions received from Karoon Gas representatives.

The following report includes tabular data of ambient permeability to air, helium injection porosity, grain density and core gamma. One sample then proceeded with special core analysis, including overburden porosity, permeability, formation factor, resistivity index and cation exchange capacity.

CHAPTER 2

SUMMARY

2. SUMMARY - MEGASCOLIDES – 1ST - STUDY OUTLINE



CHAPTER 3

ROUTINE CORE ANALYSIS

3.1 Test and Calculation Procedures

3. ROUTINE CORE ANALYSIS

3.1 Test and Calculation Procedures

3.1.1 Sample Drilling

Twelve 1½" diameter horizontal plug samples were cut at approximately 30 cm intervals throughout Core #1. Sampling sites were selected in consultation with the rig Geologist. Three vertical samples were cut at 1 metre intervals. All these samples were drilled on site using a mobile plug drill press and brine as the bit cooling and lubricating medium. On completion of drilling, the samples were tightly wrapped in Saran Wrap and sealed in air tight jars to avoid pore fluid loss.

A further eight horizontal and four vertical core plugs were cut, once the core arrived in the laboratory. All plugs were trimmed to right cylinders of standard length and off-cuts labelled and bagged for possible future analysis.

3.1.2 Probe Permeability

Probe permeability was undertaken on core pieces at the Megascollides-1ST rig site, to provide a quick estimate of permeability.

A probe is pneumatically applied to the surface of the core at 100 psig. An 'O' ring on the tip of the probe is used to achieve a seal against the rock. Air is then forced to flow at a constant pressure through the probe tip into the core and back into the atmosphere. The flow rate is measured by a series of precision flow meters which are selected to cover a wide range of flow rates. The measured flow rate (at a fixed injection pressure) is converted to permeability by comparison against measurements on core plugs with known permeabilities.

Due to the nature of the core, and high fluid saturations, no gas flow could be determined.

3.1.3 Continuous Core Gamma

The core was laid out according to depth markings, and a continuous core gamma trace produced by passing the core beneath a gamma radiation detector. The detector is protected from extraneous radiation by a lead tunnel. The detector signal is amplified and digitised to produce a gamma trace for comparison with the down hole log.

3.1.4 Core Slabbing

Upon completion of core plug drilling the core was slabbed longitudinally into two sections (1/3 : 2/3) using brine as the blade cooling and lubricating medium.

3.1.5 Dean-Stark Residual Fluid Saturation

The fresh state samples were placed into the Dean-Stark fluid extraction apparatus, suspended above a reservoir of boiling toluene. The solvent vapours, together with the extracted pore fluids, are condensed at the top of the glassware and the water collected in a calibrated side arm. Oil and toluene are collected in the reservoir and continue boiling, so that clean toluene vapour continues extracting pore fluids. The process is continued until the water production ceases.

From the collected water volume and the latter determined helium injection pore volume of the sample, the water saturation is calculated as follows:

$$S_w = \frac{\text{Pore Water Volume}}{\text{Pore Volume}} \times 100$$

Oil saturations are determined via sample weight loss during analysis and assumptions of 5800 ppm brine composition and 0.85 g/cm³ oil density.

3.1.6 Salt Extraction Analysis

Two samples were selected for salt extraction by refluxing the sample over a reservoir of boiling methanol. Solvent vapours extract residual salt (not removed during Dean-Stark analysis) and concentrate it in the methanol reservoir. After 24 hours of extraction time, the methanol solution volume was accurately determined and sent to a NATA-certified laboratory for cation analysis. Results were then corrected to the volume of water extracted from each core plug.

One extra plug sample was drilled and crushed to grain size. Salt was then dissolved in distilled water for 48 hours. The solution was filtered and solution analysed by a NATA certified laboratory. Results were then corrected based on average water saturations of plug samples from similar depths.

3.1.7 Cleaning and Drying

Quick Look Samples

Cleaning was performed in a modified soxhlet system (Appendix II) using a 3:1 chloroform:methanol azeotrope. Samples were cleaned for 17 hours to remove the majority of salt and oil. Drying was performed in a dry oven at 105°C for 15 hours. Samples were cooled to room temperature in air tight containers and proceeded with porosity and permeability determination.

Routine Core Analysis Samples

Selected samples from the Quick Look set and all dry plugs used for Dean-Stark were placed into a modified soxhlet system using a 3:1 chloroform:methanol azeotrope. Cleaning continued until tests for oil (fluorescence under UV light) and salt (silver nitrate precipitation) showed negative. The clean samples were dried to constant weight in a humidity oven at 60°C and 40% relative humidity. Once dry, samples were cooled to room temperature in an air tight chamber.

3.1.8 Porosity

The clean and dry plugs were sealed in a matrix cup and a known volume of helium at 100 psi reference pressure was introduced to the cup. From the resultant pressure, the unknown volume, i.e. the grain volume, was calculated using Boyles Law.

The bulk volume of each plug was determined by mercury immersion. The difference between the grain volume and the bulk volume was the pore volume. The porosity was calculated as the volume percentage of pore space with respect to the bulk volume.

$$\Rightarrow \begin{array}{lcl} P_1 V_1 & = & P_2 V_2 \\ P_1 V_r & = & P_2 (V_r + V_c - V_g) \end{array}$$

$$V_p = V_b - V_g$$

$$\text{Ambient Porosity \%} = \frac{V_p}{V_b} \times 100\%$$

<i>where</i>	P_1	=	<i>initial pressure (psig)</i>
	P_2	=	<i>final pressure (psig)</i>
	V_r	=	<i>reference cell volume (cm³)</i>
	V_c	=	<i>matrix cup volume (cm³)</i>
	V_g	=	<i>grain volume (cm³)</i>
	V_p	=	<i>pore volume (cm³)</i>
	V_b	=	<i>bulk volume (cm³)</i>

3.1.9 Permeability to Air

The plugs were placed in a Hassler cell at a confining pressure of 250 psig. This pressure was used to prevent bypassing of air around the sample when the measurement is made.

During the measurement, a known air pressure was applied to the upstream face of the sample, creating a flow of air through the sample. Permeability for each sample was then calculated using Darcy's Law, through knowledge of the upstream pressure and flow rate during the test, the viscosity of air and the plug dimensions.

$$Ka = \frac{2000.BP.\mu.q.L}{(P_1^2 - P_2^2).A}$$

<i>where</i>	<i>Ka</i>	=	<i>air permeability (milliDarcys)</i>
	<i>BP</i>	=	<i>barometric pressure (atmospheres)</i>
	<i>μ</i>	=	<i>gas viscosity (cP)</i>
	<i>q</i>	=	<i>flow rate (cm³/s) at barometric pressure</i>
	<i>L</i>	=	<i>sample length (cm)</i>
	<i>P₁</i>	=	<i>upstream pressure (atmospheres)</i>
	<i>P₂</i>	=	<i>downstream pressure (atmospheres)</i>
	<i>A</i>	=	<i>sample cross sectional area (cm²)</i>

3.1.10 Apparent Grain Density

The apparent grain density was calculated by dividing the weight of the plug by the grain volume determined from the helium injection porosity measurement.

$$\rho = \frac{Wt}{Vg}$$

<i>where</i>	<i>ρ</i>	=	<i>grain density (g/cm³)</i>
	<i>Wt</i>	=	<i>weight of sample (g)</i>
	<i>Vg</i>	=	<i>grain volume (cm³)</i>

3.1.11 Core Photography

Core photography was carried out on the 2/3 slab of core using a Nikon D100 6.1 megapixel digital SLR camera. Photographs were taken of the core in 5 m format under white light and ultra violet light. These photographs have been digitally edited and core plug data inserted.

CHAPTER 3

ROUTINE CORE ANALYSIS

3.2 Test Results

3.2.1 Ambient Test Results

AMBIENT TEST RESULTS

Client : Karoon Gas Australia Ltd
Well : Megascolides-1ST
Core Int : 1881.00m - 1887.60m
Core Int : 1887.60m - 1892.60m

Date : 16/01/2007
File : 0387-02
Analysts : kw, dg, ag, dn

Sample Number	Depth	Dir	Quick Look			Soxhlet Clean & Humidity Dry			Fluid Saturation So	Remarks
			Soxhlet Clean (17hr) Oven Dry (15hr)		Permeability to Air	Porosity Helium	Grain Density			
			Porosity Helium	Grain Density						
								Permeability to Air		
	(m)		(percent)	(g/cm ³)	(mD)	(percent)	(g/cm ³)	(mD)	(percent)	(percent)
1	1883.55	H	2.8	2.70	0.06					
2	1883.78	H	5.1	2.68	0.06					
1V	1883.95	H				6.8	2.68	0.09	0.7	97.1
7V	1884.05	H				6.6	2.67	0.05	10.5	86.4
3	1884.40	H	5.9	2.70	0.12					
4	1884.67	H	8.7	2.69	0.37					
5	1884.92	H	6.8	2.70	0.64					
2V	1885.05	H				8.2	2.67	0.24	0.7	92.7
6	1885.20	H	10.9	2.67	0.65					
7	1885.50	H	10.7	2.68	0.97	10.4	2.67	0.77		
S1	1885.69	H				11.5	2.68	0.56		
8	1885.84	H	11.4	2.66	0.65					
3V	1885.98	H				9.2	2.67	0.47	10.1	89.1
9	1886.07	H	10.9	2.66	0.54					

Sample Number	Depth	Dir	Quick Look			Soxhlet Clean & Humidity Dry			Fluid Saturation		Remarks
			Soxhlet Clean (17hr) Oven Dry (15hr)			Soxhlet Clean & Humidity Dry			So	Sw	
			Porosity	Grain	Permeability	Porosity	Grain	Permeability			
			Helium	Density	to Air	Helium	Density	to Air			
	(m)		(percent)	(g/cm ³)	(mD)	(percent)	(g/cm ³)	(mD)	(percent)	(percent)	
10	1886.29	H	10.1	2.68	0.88	10.2	2.69	0.77			
11	1886.60	H	10.9	2.68	0.42						
4V	1886.80	H				9.4	2.68	0.24	0.7	96.5	
12	1887.10	H	8.7	2.68	0.09						
13	1887.35	H	6.0	2.70	0.02						
14	1887.96	H	3.8	2.69	0.01	4.3	2.70	0.01			
5V	1888.05	H				3.8	2.69	0.06	2.8	76.7	
15	1888.25	H	3.2	2.70	0.02	3.4	2.70	0.02			
16	1888.66	H	3.7	2.68	0.01						
17	1888.89	H	4.9	2.69							Irregular
18	1889.30	H	3.7	2.70	0.04						
6V	1889.52	H				4.1	2.70	0.02	24.9	72.5	
19	1889.64	H	4.7	2.65	0.05	4.9	2.65	0.05			
20	1889.95	H				6.0	2.67	0.06	37.1	55.6	

CHAPTER 3

ROUTINE CORE ANALYSIS

3.2 Test Results

3.2.2 Water Analysis

WATER ANALYSIS

Client : Karoon Gas Australia Ltd

Well : Megascollides-1ST

Sample Number	Depth (m)	Sample Volume (mL)	Total Salt				Water Composition			
			Calcium (mg/L)	Magnesium (mg/L)	Sodium (mg/L)	Potassium (mg/L)	Calcium (mg/L)	Magnesium (mg/L)	Sodium (mg/L)	Potassium (mg/L)
Distilled Water			0.037	0.001	1.668	5.174				
W1	1885.34	39	2.396	0.035	114.259	5.169	†	47.2	0.68	2252
Mud Filtrate								129	2.72	2650
										9830
Methanol Blank			0.072	0.002	0.377	0.242				
3V	1885.98	106	0.372	0.011	10.694	0.249	‡	3.61	0.08	2243
4V	1886.80	112	0.200	0.004	9.012	0.240	‡	1.45	0.02	1919

† Water analysis was performed on a crushed plug sample and salt extracted by distilled water.

‡ On completion of water extraction by Dean Stark salt was removed by refluing the sample with Methanol

Based on average of results water composition is 5800 ppm giving an Rw of 0.98 ohm.m

CHAPTER 3

ROUTINE CORE ANALYSIS

3.2 Test Results

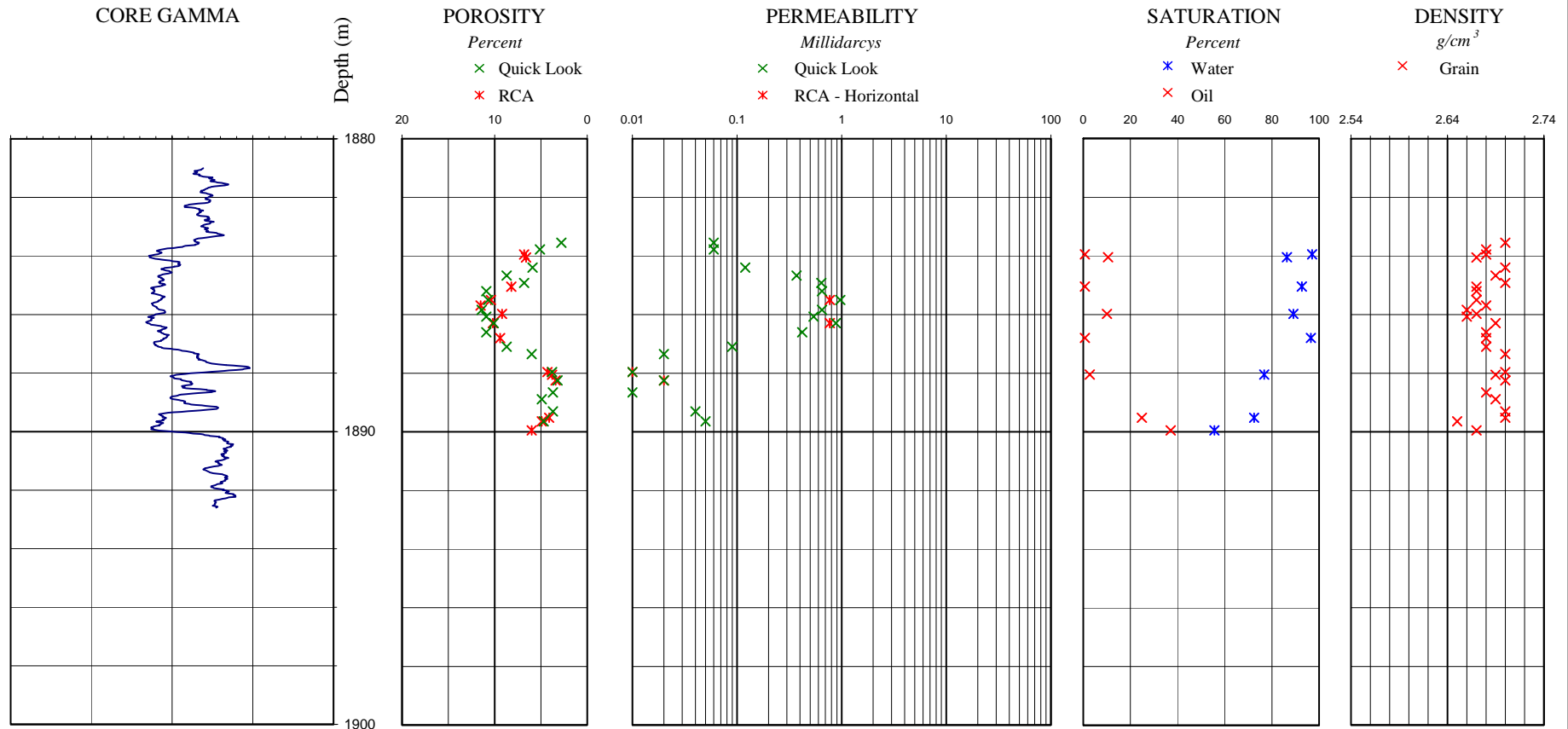
3.2.3 Core Log Plot

CORE PLOT



Client: Karoon Gas Australia Ltd
Well: Megascollides-1ST
File No.: 0387-02

Core Int: 1881.00m - 1887.60m
Core Int: 1887.60m - 1892.60m



CHAPTER 4

ELECTRICAL PROPERTIES

4.1 Test and Calculation Procedures

4. ELECTRICAL PROPERTIES

4.1 Test and Calculation Procedures

4.1.1 Base Parameters at Overburden Pressure

Overburden base parameters were performed by placing the selected sample into an individual thick-walled rubber sleeve and loading assembly into a hydrostatic cell.

With an ambient pressure (400 psi) applied to the sample, helium held at 100 psi reference pressure was released into the samples pore volume. The resultant pressure drop was used to determine pore volume at ambient. The confining pressure was then increased to the overburden pressure of 3600 psi and the resultant change in internal pore pressure was monitored and used to determine pore volume at overburden conditions.

$$\text{Overburden Porosity \%} = \frac{V_p - \Delta V_p}{V_b - \Delta V_p} \times 100$$

$$\begin{array}{lll} \text{where} & V_p & = \text{ambient pore volume (cm}^3\text{)} \\ & V_b & = \text{ambient bulk volume (cm}^3\text{)} \\ & \Delta V_p & = \text{change in pore volume (cm}^3\text{)} \end{array}$$

Whilst at overburden pressure, permeability was determined using procedures as described in Section 3.1.9 of this report.

4.1.2 Sample Saturation

A 5800 ppm brine was prepared by ACS Laboratories (Appendix I) and pre-filtered to 0.45 μ m.

The selected sample was initially vacuum saturated with brine followed by pressure saturation at 2000 psi for a minimum of 12 hours. To determine complete saturation, the pore volume of the sample was ascertained by mass balance and compared with that determined by porosimetry.

4.1.3 Formation Resistivity Factor

The fully brine saturated sample was sandwiched between a pair of stainless steel core holder platens. These platens also act as the current carrying and potential electrodes. A thin silver leaf was also placed between the plug endfaces and electrodes, to ensure electrical contact. A strongly hydrophilic membrane was placed at the bottom end of the sample. This assembly was placed into a snugly fitting rubber overburden sleeve and then loaded into a Hydrostatic type core holder. A confining pressure was gradually applied as an effective overburden pressure (see Appendix II for schematic).

Synthetic brine (Appendix I) was slowly flowed through the sample at a rate of 0.5 cm³/min. During this process sample resistivity was monitored on a digi-bridge capable of measuring sample resistance to 0.001 (ohms) accuracy. In each case the current frequency was selected to yield minimum phase angles, thus ensuring maximum electrical contact (between each sample and the current carrying and potential electrodes). Values of sample resistance (Rc) and effluent brine resistivity (Rw) were recorded daily. Each sample was deemed to be at ionic equilibrium when three consecutive daily readings were recorded within 1%.

From these stable data, the following results were recorded:

$$Ro = \frac{A \cdot Rc}{100L}$$

where

<i>Ro</i>	=	<i>sample resistivity (ohm.m)</i>
<i>Rc</i>	=	<i>sample resistance (ohms)</i>
<i>L</i>	=	<i>electrode gap (sample length - cm)</i>
<i>A</i>	=	<i>cross sectional area (cm²)</i>
<i>100</i>	=	<i>units conversion</i>

Formation resistivity factor was calculated using the following equations:

$$FF = \frac{a}{\Phi^m}$$

and

$$FF = \frac{Ro}{Rw}$$

where

<i>Rw</i>	=	<i>brine resistivity (ohm.m)</i>
<i>a</i>	=	<i>intercept (assumed = 1)</i>
<i>m</i>	=	<i>cementation exponent</i>

and

<i>Φ</i>	=	<i>porosity (fraction)</i>
----------	---	----------------------------

The brine resistivity (Rw) was accurately determined by a NATA certified fluids laboratory.

4.1.4 Continuous Injection Resistivity Index

Upon completion of the preceding formation factor analyses, the sample continued immediately for resistivity index analyses. The top endface port was connected to a supply of isopar oil and the bottom port connected to a graduated receiving tube. The sample was desaturated by pumping oil into each sample at a fixed rate so desaturation proceeded over a 14 day period. A small amount of oil was placed into the collection tube to prevent any potential brine loss by evaporation. Sample resistances (Rc) were measured at regular decreasing brine saturations. The saturation values were calculated from the following equation based on produced volumes:

$$\text{Water Saturation (\%)} = \frac{\text{Pore Volume @ OB (cm}^3\text{)} - \text{Brine Expelled (cm}^3\text{)}}{\text{Pore Volume @ OB (cm}^3\text{)}} \times 100$$

The ratio of the sample resistance (Rc) values to the previously determined FF values (at 100% saturation) were used to calculate the formation resistivity indices, (i.e. comparing the resistivity of the partially saturated to that of the fully saturated sample).

$$R_t = \frac{A \cdot R_c}{100L}$$

where R_c = sample resistance (ohms)
 R_t = resistivity of partially brine saturated sample (ohm.m)
 100 = units conversion
 L = electrode gap (sample length – cm)
 A = cross sectional area (cm²)

$$\text{and } RI = \frac{R_t}{R_w \cdot FF}$$

where R_w = resistivity of brine (ohm.m)
 FF = formation factor

(This equation was modified from the standard Archie equation to incorporate the variable brine resistivity which is temperature dependent.)

These RI values (for each sample) were plotted against brine saturation (Sw) on graphs with logarithmic axes and the gradient of the best-fit line through the coordinate (1.0, 1.0) was calculated. Each gradient is quoted as the saturation exponent (n) for that sample, in accordance with Archie's formula.

$$RI = \frac{1}{S_w^n}$$

On completion, terminal water saturations were confirmed by Dean-Stark analysis.

4.1.5 Cation Exchange Capacity

Cation exchange capacity was determined on approximately 5 grams of sample (off-cut) using the wet chemistry method. The sample was first washed with an ammonium chloride solution to exchange ions with the available clay cations. An exchange reagent was then washed through the sample and the resultant solution titrated. Where a smaller sample is used the limit of detection becomes greater and a minimum value is reported.

Values of exchangeable cations (theoretical minimum of zero) present in the samples are reported as milliequivalents per 100 grams of dry sample (meq/100 g). Values of Q_v have been calculated using the following equation:

$$Q_v = \frac{CEC (1 - \Phi) \rho}{100 \Phi}$$

where

$$\begin{aligned} \rho &= \text{grain density (g/cm}^3\text{)} \\ \Phi &= \text{porosity (fraction)} \\ Q_v &= \text{volume concentration of clay exchange cations} \\ &\quad \text{(meq/cm}^3 \text{ pore space)} \\ CEC &= \text{cation exchange capacity (meq/100 g dry sample)} \end{aligned}$$

Based on these CEC/ Q_v data, values of shaly sand equivalent formation factor (FF^*), cementation factor (m^*) and saturation exponent (n^*) were calculated using the following equations:

$$FF^* = FF \cdot (1 + B \cdot Q_v \cdot R_w)$$

$$m^* = \frac{\log FF^*}{-\log \Phi}$$

$$n^* = \frac{\log \left[\frac{1 + R_w \cdot B \cdot Q_v}{1 + R_w \cdot B \cdot Q_v / S_w} \right] - \log FRI}{\log S_w}$$

$$\text{where}^1 B = \frac{-1.28 + 0.225 \cdot T - 0.0004059 \cdot T^2}{1 + R_w^{1.23} \cdot (0.045 \cdot T - 0.27)}$$

$$\begin{aligned} FF &= \text{formation resistivity factor} \\ FF^* &= \text{shaly sand equivalent formation resistivity factor} \\ m^* &= \text{shaly sand equivalent cementation factor} \\ \Phi &= \text{porosity (fraction)} \\ n^* &= \text{shaly sand equivalent saturation exponent} \\ R_w &= \text{brine resistivity (ohm.m @ 25}^\circ\text{C)} \\ T &= \text{temperature of 25}^\circ\text{C} \\ B &= \text{equivalent conductance of clay exchange cations} \\ Q_v &= \text{volume concentration of clay exchange cations} \\ S_w &= \text{final saturation (fraction)} \\ FRI &= \text{resistivity index @ saturation } S_w \end{aligned}$$

¹ Juhasz, I., 1981, Normalized Q_v - the key to shaly sand evaluation using the Waxman-Smiths equation in the absence of core data, paper Z, in 22nd Annual Logging Symposium Transactions: Society of Professional Well Log Analysts, 36p.

CHAPTER 4

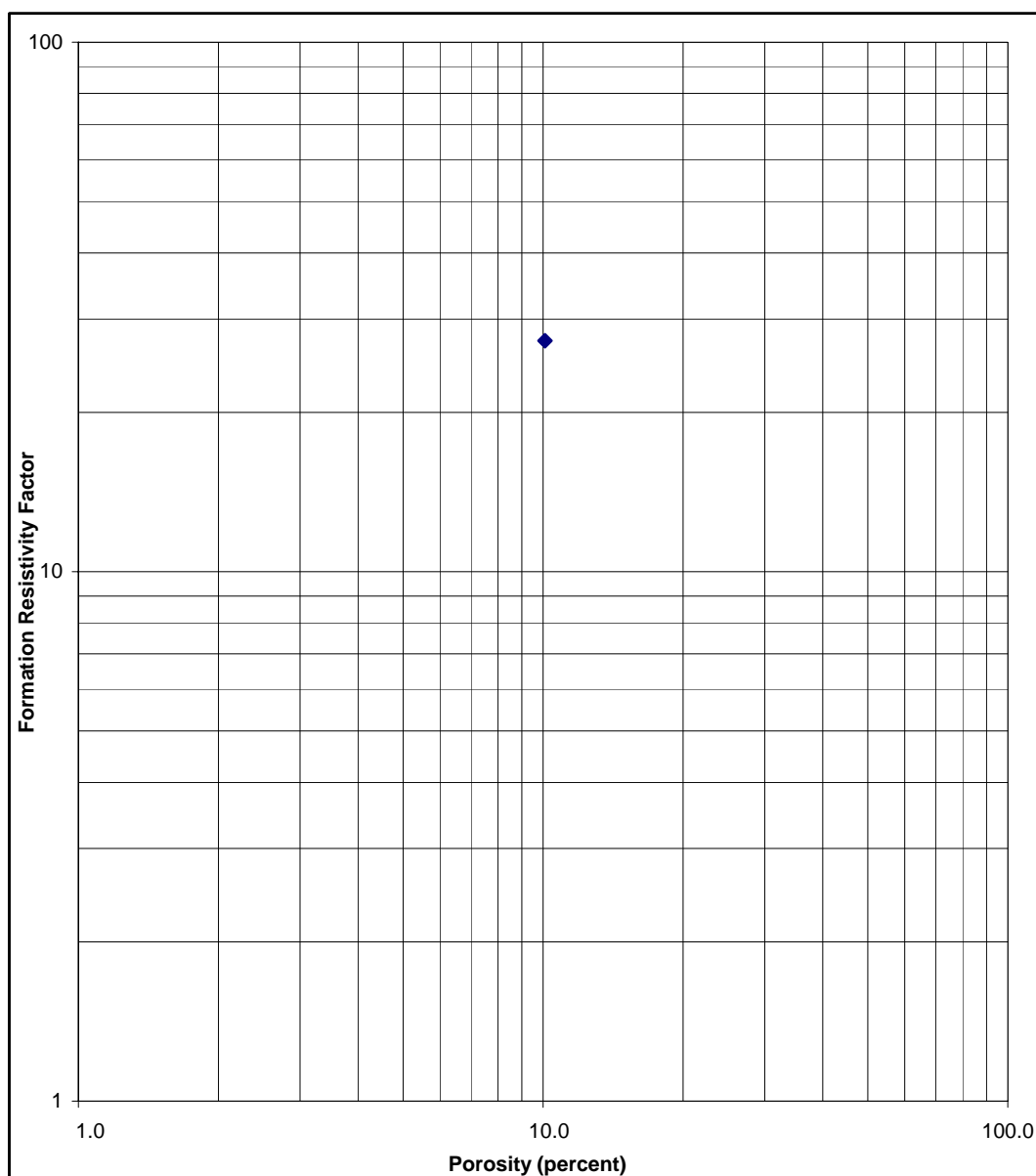
ELECTRICAL PROPERTIES

4.2 Test Results

FORMATION RESISTIVITY FACTOR

Client	Karoo Gas Australia	Saturant	5800 ppm
Well	Megascolides-1ST	Rw of Saturant	1.02 at 25°C
		Overburden	3600 psi
		Average m	1.44

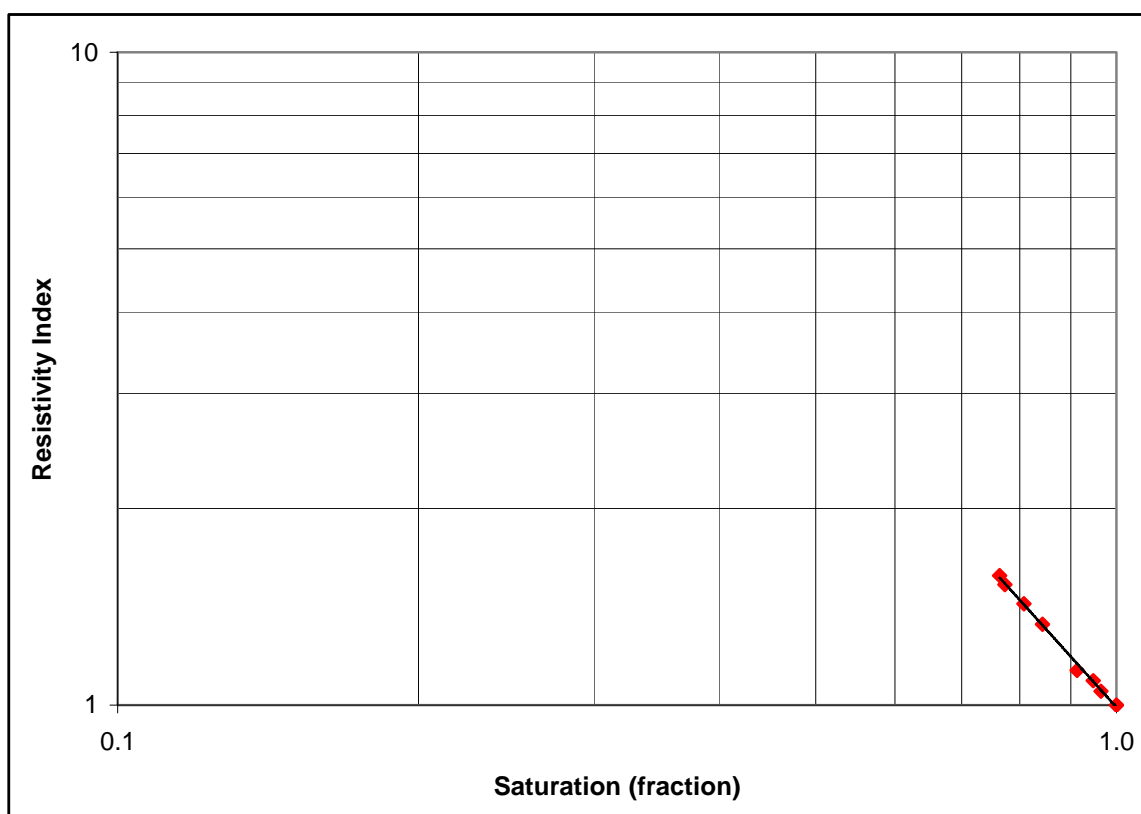
Sample Number	Depth (metres)	Permeability to Air (milliDarcy's)	Porosity (percent)	Formation Factor FF	Cementation Exponent m
S1	1885.69	0.07	10.1	27.3	1.44



RESISTIVITY INDEX

Client Karoon Gas Australia
Well Megascolides-1ST
Rw of Saturant 1.02 at 25°C
Method Continuous Injection @ Overburden

Sample Number	Depth (metres)	Permeability to Air (milliDarcy's)	Porosity (percent)	Formation Factor FF	Brine Saturation (fraction)	Resistivity Index RI	Saturation Exponent n
S1	1885.69	0.07	10.1	27.3	1.000	1.00	1.64
					1.000	1.00	
					0.965	1.05	
					0.948	1.09	
					0.913	1.13	
					0.843	1.33	
					0.808	1.43	
					0.773	1.53	
					0.764	1.58	



CATION EXCHANGE CAPACITY

Client Karoon Gas Australia
Well Megascolides-1ST

Sample Number	Depth (metres)	Porosity (percent)	Grain Density (g/cm ³)	Cation Exchange Capacity (meq/100g)		Quantity of Cation Exchangeable Clay Qv (meq/cm ³)	
				Uncrushed	Crushed	Uncrushed	Crushed
S1	1885.69	11.5	2.68	2.67	5.72	0.55	1.18

FORMATION RESISTIVITY FACTOR

Client	Karooon Gas Australia	Rw of Saturant	1.02 at 25°C
Well	Megascalides-1ST	Overburden	3600 psi

Sample Number	Depth (metres)	Permeability to Air (milliDarcy's)	Porosity (percent)	Formation Factor FF	Cementation Exponent m	Saturation Exponent n	Shaley Sand Equivalent		
							Formation Factor FF*	Cementation Exponent m*	Saturation Exponent n*
S1	1885.69	0.07	10.1	27.3	1.44	1.64	64.3	1.82	2.23

CHAPTER 5

SAMPLE DISTRIBUTION AND STORAGE

5. SAMPLE DISTRIBUTION AND STORAGE

The 1/3 and 2/3 slabs of core are currently stored at ACS Laboratories' Brisbane facility awaiting instructions to send to the Department of Primary Industries core store in Werribee.

All core plugs and off-cuts are to be returned to Karoon Gas' Collins Street offices.

APPENDIX I

FLUID PROPERTIES

FLUID PROPERTIES

5800 ppm NaCl Equivalent Brine

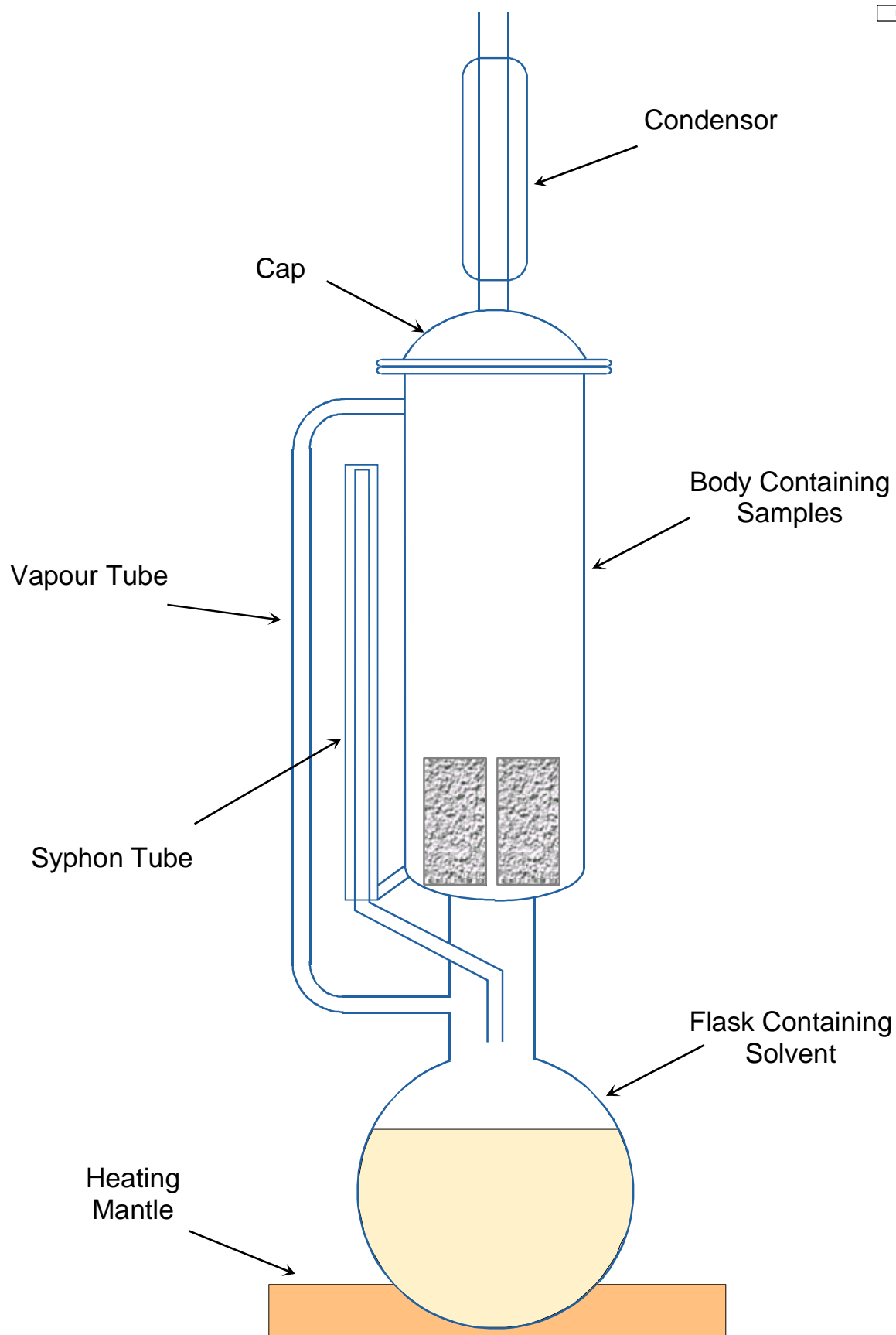
Density = 1.00 g/cm³ @ 25°C

Resistivity = 1.02 ohm.m @ 25°C

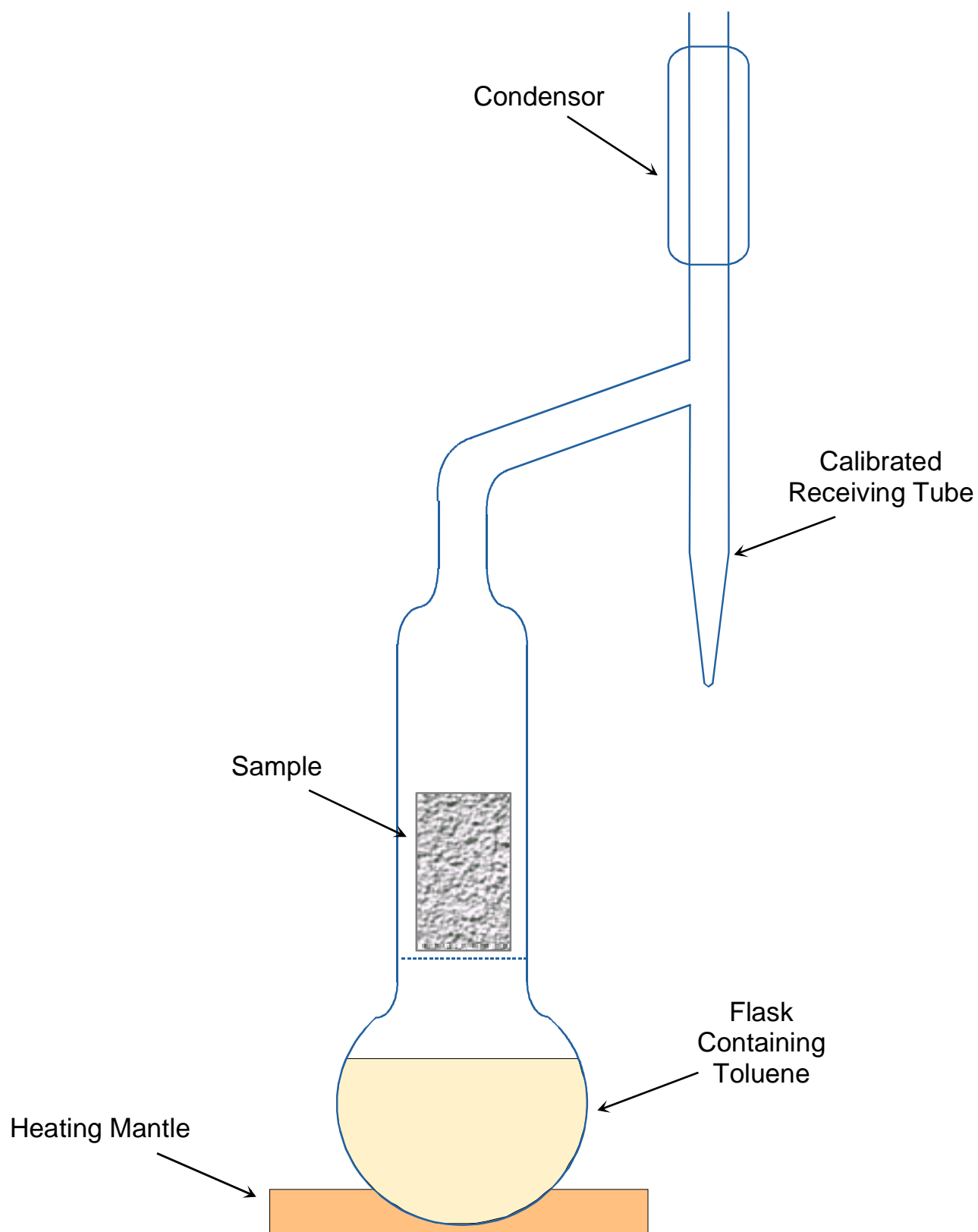
APPENDIX II

EQUIPMENT SCHEMATICS

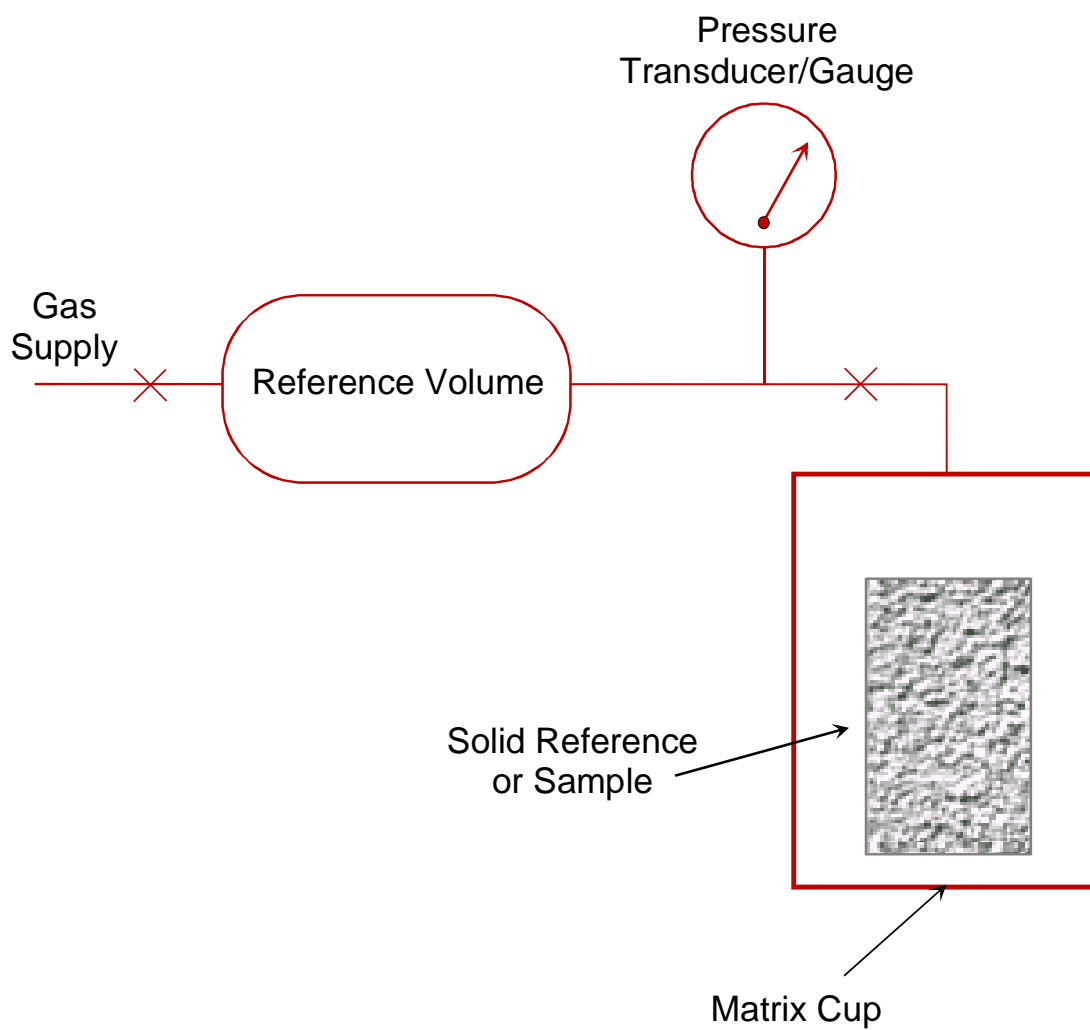
SOXHLET CLEANING APPARATUS



DEAN-STARK APPARATUS

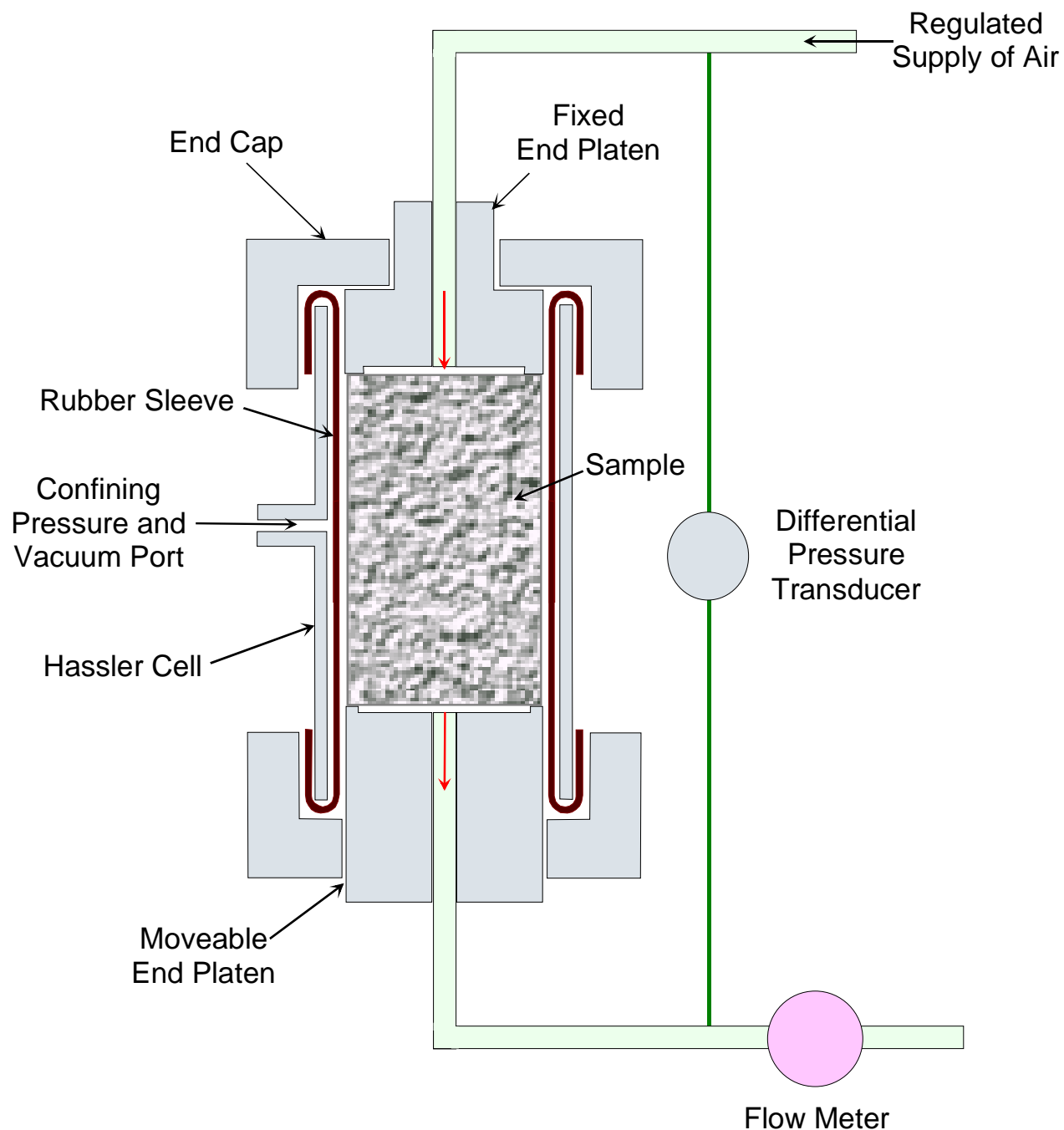


POROSIMETER SCHEMATIC

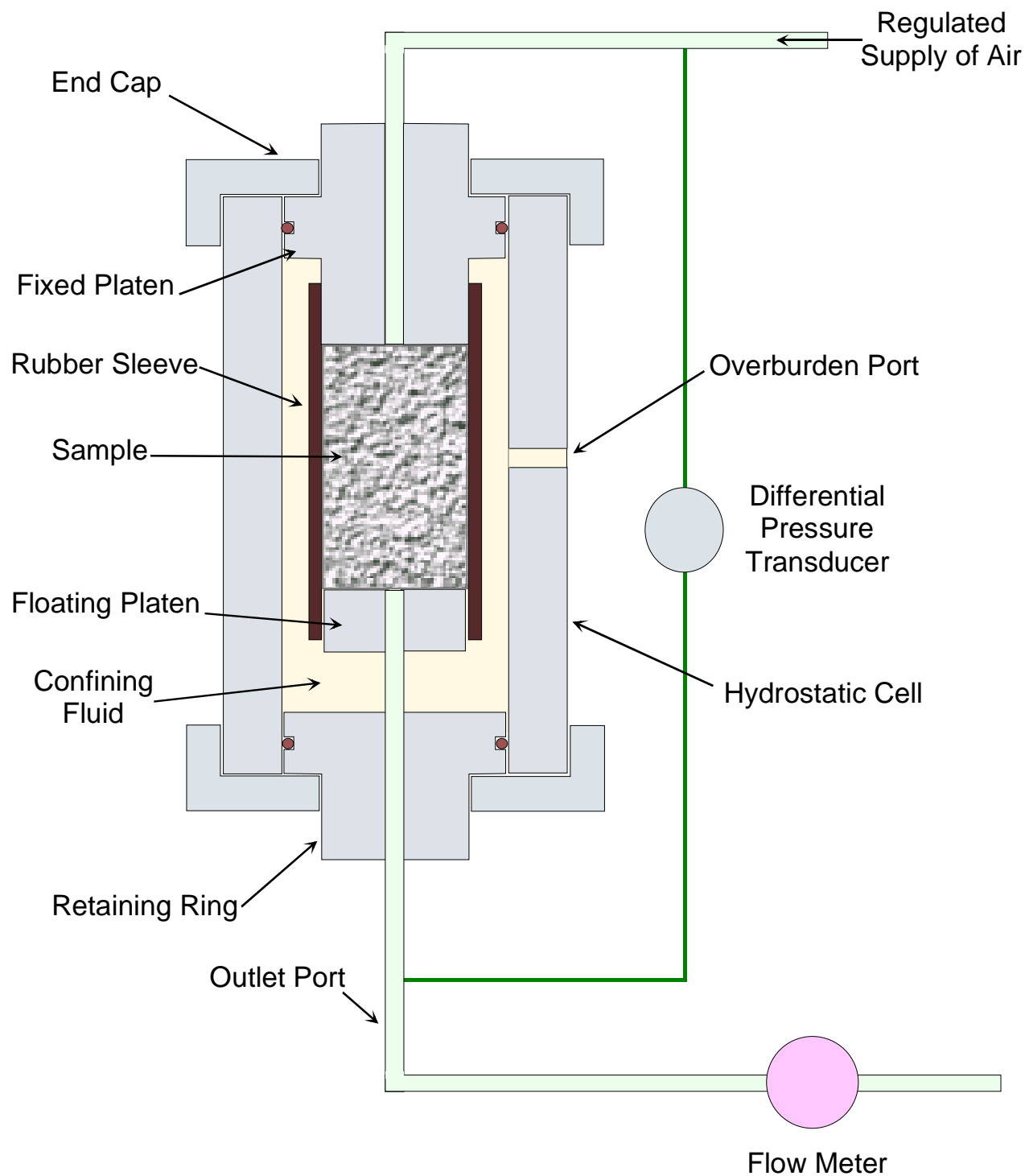


$$P1.V1 \text{ (reference)} = P2.V2 \text{ (sample)}$$

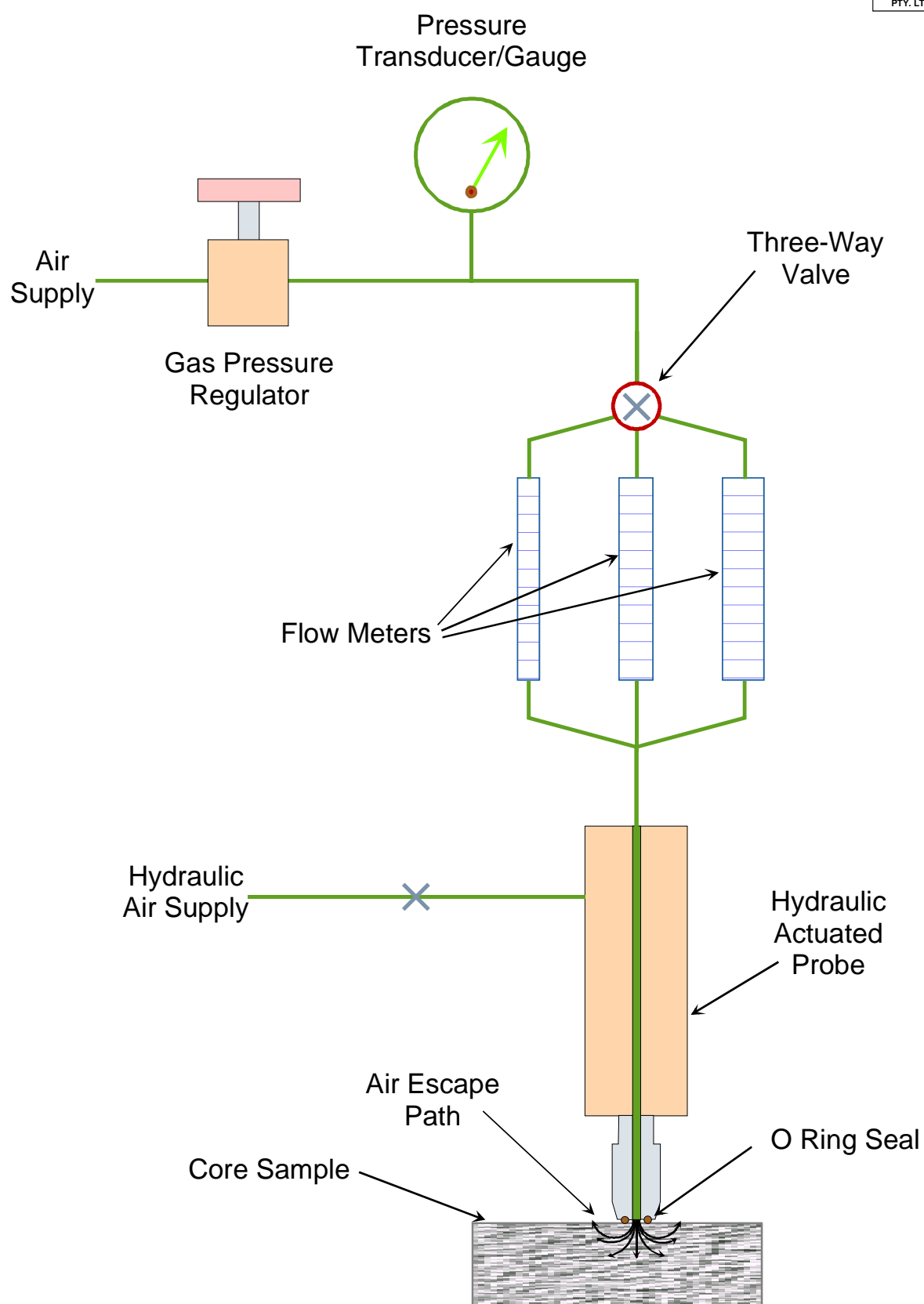
GAS PERMEAMETER SCHEMATIC (Hassler)



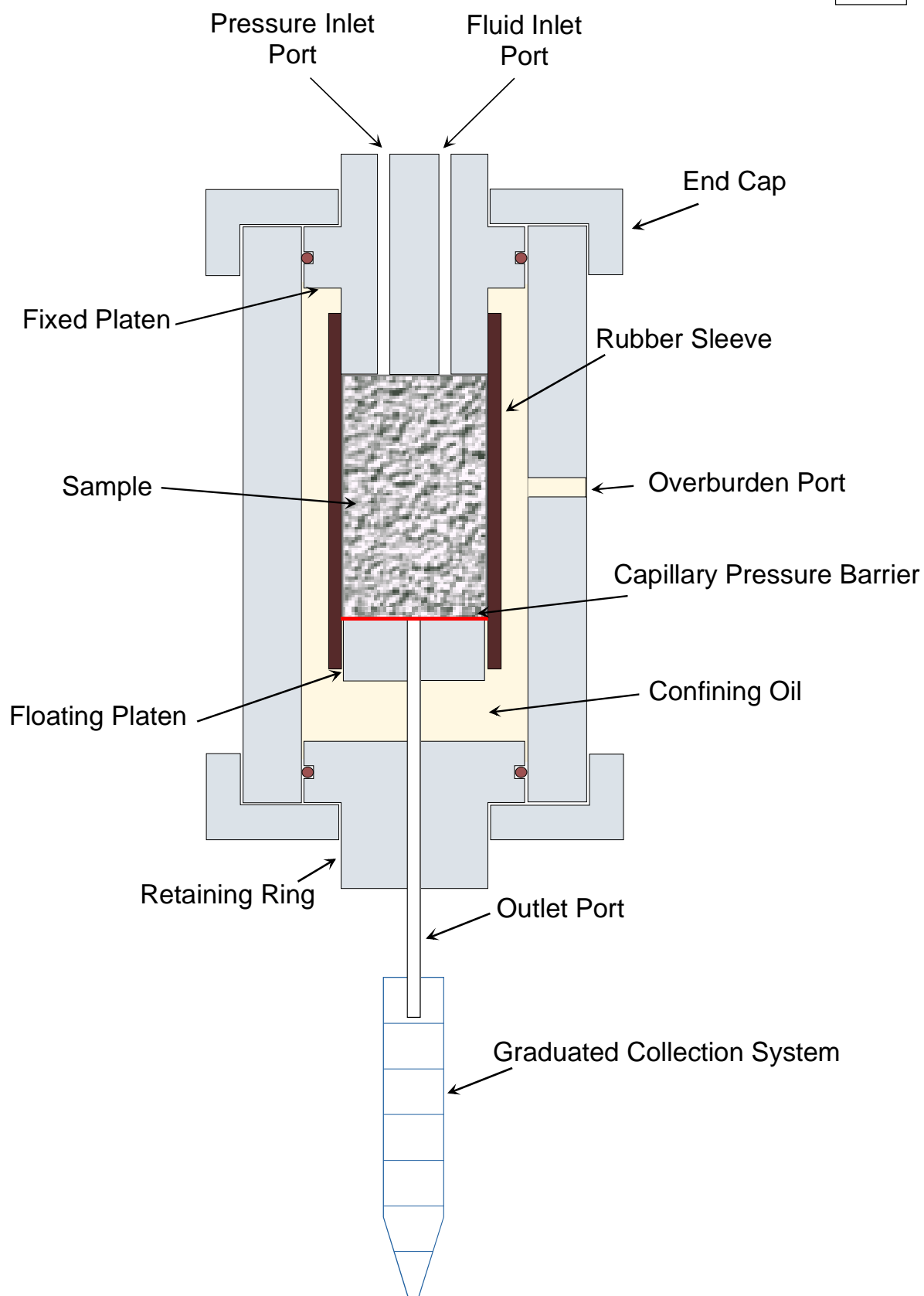
GAS PERMEAMETER SCHEMATIC (Hydrostatic)



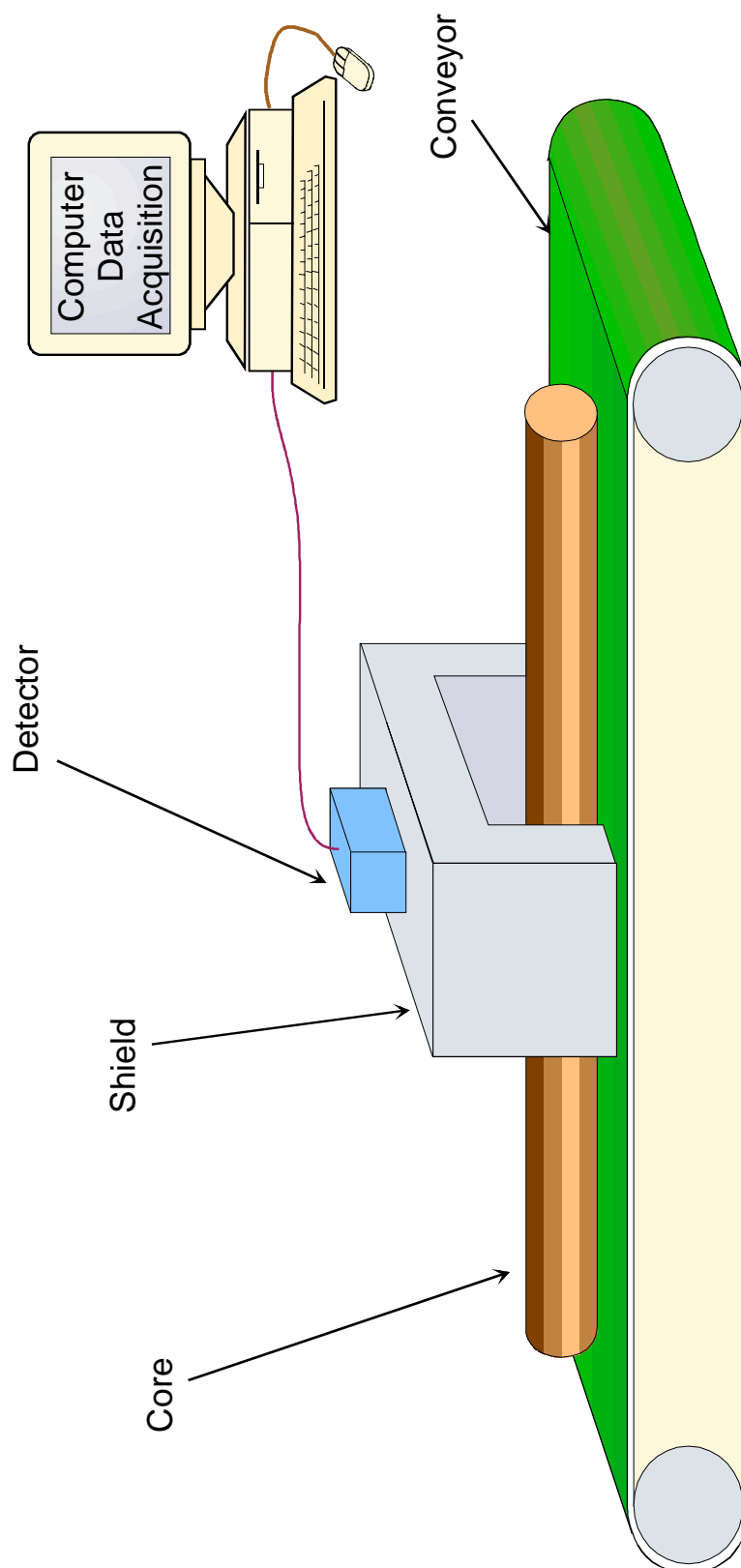
PROBE PERMEAMETER SCHEMATIC



HYDROSTATIC CAPILLARY PRESSURE CELL



CONTINUOUS CORE GAMMA SCHEMATIC



APPENDIX III

PETROLOGY REPORT



PETROLOGY
of
MEGASCOLIDES-1ST CORE SAMPLES
for
KAROON GAS AUSTRALIA LTD
by
ACS LABORATORIES PTY LTD



20 February, 2007

Karoo Gas Australia Ltd
Level 9, 406 Collins Street
MELBOURNE VIC 3000

Attention: Lino Barro

FINAL REPORT: 0519-01 – MEGASCOLIDES-1ST

CLIENT REFERENCE: PO 249

MATERIAL: Two core samples

LOCALITY: Megascolides-1ST

WORK REQUIRED: Petrology

Please direct technical enquiries regarding this work to the signatory below under whose supervision the work was carried out.

NICK COX
Operations Manager

ACS Laboratories Pty Ltd shall not be liable or responsible for any loss, cost, damages or expenses incurred by the client, or any other person or company, resulting from any information or interpretation given in this report. In no case shall ACS Laboratories Pty Ltd be responsible for consequential damages including, but not limited to, lost profits, damages for failure to meet deadlines and lost production arising from this report.

Head Office: 8 Cox Road, Windsor Qld 4030, Australia
☎: 61 7 3357 1133 Facsimile: 61 7 3357 1100
E-mail: info@acslabs.com.au

ACS Laboratories Pty Ltd
ABN: 81 008 273 005

PETROLOGY

of

MEGASCOLIDES-1ST CORE SAMPLES

A report prepared for

KAROON GAS AUSTRALIA LTD

by

JULIAN C. BAKER Ph.D.

February 2007

CONTENTS

	Page
EXECUTIVE SUMMARY	1
1. INTRODUCTION	2
2. ANALYTICAL PROGRAM	
2.1 Thin-Section Analysis	2
2.2 X-Ray Diffraction Analysis	2
2.3 Scanning Electron Microscopy	2
3. THIN-SECTION DESCRIPTIONS	3
4. X-RAY DIFFRACTION ANALYSES	7
5. SUMMARY AND CONCLUSIONS	9

TABLES

TABLE 1. THIN-SECTION AND CORE ANALYSES	4
TABLE 2. BULK-ROCK XRD ANALYSES	8
TABLE 3. FINE-FRACTION CLAY MINERALOGY	8

FIGURES

FIGURE 1. QFR COMPOSITIONS	5
---	----------

APPENDICES

- 1. X-RAY DIFFRACTION TRACES**
- 2. MICROGRAPHS**

EXECUTIVE SUMMARY

A petrological study was carried out on two core samples from 1885.50m and 1889.64m in Megascollides-1ST. Analytical techniques used were thin-section analysis, quantitative bulk-rock/fine-fraction X-ray diffraction analysis, and scanning electron microscopy.

Samples are a poorly sorted, very coarse grained feldspathic litharenite (1885.50m) and an argillaceous, moderately sorted, coarse grained lithic arkose (1889.64m) in which framework grains are mainly quartz, plagioclase and a variety of rock fragments.

Sandstones are derived from a polymictic continental provenance dominated by garnetiferous granodiorites and which also included siliciclastic sedimentary rocks, low-grade metasedimentary rocks and intermediate volcanic rocks.

Detrital clay is concentrated along thin laminae at 1889.64m. Authigenic kaolin forms scattered patches and patchy pseudomatrix where labile grains, particularly plagioclase, have altered. Authigenic clay also includes mixed-layer illite/smectite that is associated with some altered labile rock fragments. Clay minerals detected by XRD are kaolin and subordinate illite/mica, mixed-layer illite/smectite (60-65% illite interlayers) and chlorite.

Other diagenetic effects besides authigenic clay formation include quartz overgrowth and calcite cementation, physical compaction, grain contact dissolution/microstylolite and feldspar/garnet dissolution.

Samples contain little or no primary intergranular porosity due to the deleterious effects of advanced diagenesis. Porosity reduction at 1889.64m also results from detrital clay pore filling along argillaceous laminae. Secondary labile grain dissolution pores, being few and far between, do nothing to enhance reservoir quality.

With virtually all intergranular spaces being filled by cement, clay and compacted ductile grains, effective porosity is absent and permeabilities are consequently very low (0.77mD, 0.05mD).

1. INTRODUCTION

A petrological study was carried out on two core samples from 1885.50m and 1889.64m in Megascolides-1ST in order to determine texture, mineralogy, diagenetic effects and controls on reservoir quality.

2. ANALYTICAL PROGRAM

2.1 Thin-Section Analysis

Thin-sections were cut in kerosene and impregnated with blue-dyed epoxy resin to aid porosity recognition. In each thin-section, mineral composition and visible porosity were determined by a count of 350 points, and mean grain size and sorting were estimated with the aid of an eyepiece graticule. Photomicrographs were taken of each thin-section to illustrate texture, composition, diagenetic effects and porosity.

2.2 X-Ray Diffraction Analysis

Bulk-rock X-ray diffraction (XRD) analysis was carried out on both samples in order to quantify mineral abundance. The XRD analysis used a finely ground whole rock powder sample and the SIROQUANT processing technique was used to calculate mineral abundance.

Fine-fraction XRD analysis was carried out on both samples in order to precisely determine clay mineralogy. The fine fraction was separated from each sample by disaggregation and settling in distilled water and was air dried on glass discs to produce oriented specimens for XRD analysis. Samples were analysed in air dried condition and also following treatment with ethylene glycol.

2.3 Scanning Electron Microscopy

Scanning electron microscopy (SEM) was carried out on both samples in order to provide information on porosity characteristics and clay morphology/distribution. Analyses were done on freshly exposed surfaces that had been thoroughly washed in shellite to remove volatile hydrocarbons.

3. THIN-SECTION DESCRIPTIONS

Thin-section texture and composition are given in Table 1, and QFR compositions are plotted in Figure 1. Annotated thin-section and SEM micrographs are presented in Appendix 2.

#7 1885.50m

Plates 1-4

Texture and framework grains: Sample is a massive, grain supported, poorly sorted, very coarse grained feldspathic litharenite in which framework grains are mainly quartz, rock fragments and plagioclase and which also include heavy minerals (garnet, tourmaline, zircon) and biotite. Quartz grains are mostly subangular to subrounded (ignoring quartz overgrowths) and monocrystalline. Polycrystalline quartz includes granitic quartz, quartzite and metaquartzite. Plagioclase is fresh to strongly sericitised and locally has quartz intergrowths indicative of a granitic origin. Lithics are sedimentary rock fragments (strongly indurated silty mudrock, quartzose siltstone and very fine grained quartzose sandstone), volcanic rock fragments (altered/silicified intermediate vitric tuffs and lavas – locally with quartz and plagioclase phenocrysts), granitic rock fragments (coarsely intergrown quartz and plagioclase) and metamorphic rock fragments (quartz-mica/chlorite schist; phyllite). Widely scattered pebbles range up to 7mm long and are subangular to subrounded argillaceous sedimentary rock fragments. Garnet is particularly common as an accessory heavy mineral. The framework grain assemblage is indicative of a polymictic continental provenance dominated by garnetiferous granodiorites and which also included siliciclastic sedimentary rocks, low-grade metasedimentary rocks and intermediate volcanic rocks.

Clay: Clay is mainly authigenic kaolin that forms large, widely scattered microcrystalline patches where plagioclase, labile rock fragments and micaceous grains have partly to completely altered. Clay also includes authigenic mixed-layer illite/smectite that is associated with some altered labile rock fragments.

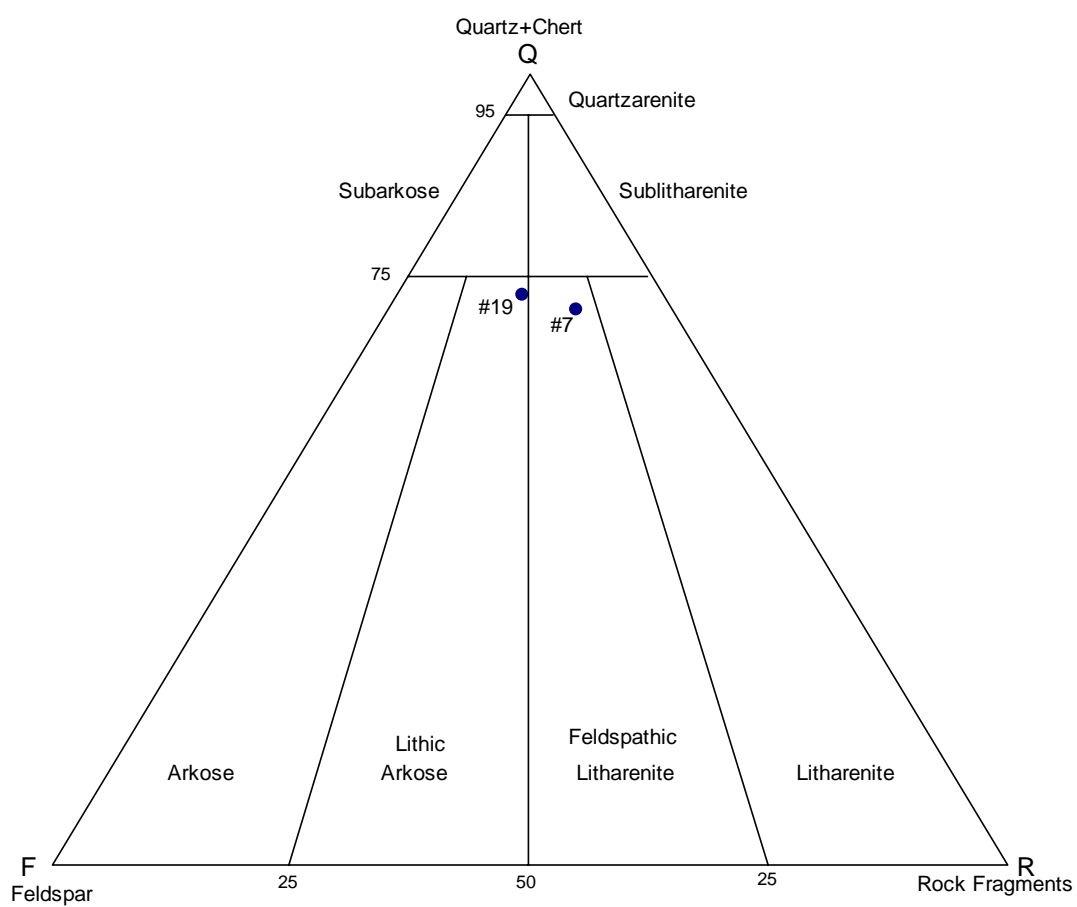
Diagenesis: The sandstone is strongly cemented by quartz overgrowths, which, between groups of quartz grains, completely fill intergranular spaces to form triple point grain contacts. Quartz overgrowths are easily distinguished from their detrital grain hosts by dustriums that are defined by thinly-developed, grain-coating leucoxene and clay. Cement also includes late-stage, coarsely-crystalline calcite, which not only sporadically infills intergranular pores and intragranular microfractures, but also commonly replaces plagioclase and sedimentary rock fragments. Calcite fills intergranular pores that were incompletely filled by quartz overgrowths at the time of calcite cementation, indicating that calcite cementation occurred during quartz overgrowth cementation. Other diagenetic effects besides quartz overgrowth and calcite cementation include grain contact dissolution, authigenic kaolin formation, ductile grain/authigenic clay compaction, plagioclase/garnet dissolution to form secondary porosity, and anatase precipitation. Quartz overgrowths enclose authigenic kaolin and penetrate secondary grain dissolution pores, indicating that quartz overgrowths postdate kaolin and secondary porosity.

TABLE 1. THIN-SECTION AND CORE ANALYSES

Sample #	7	19
Depth (m)	1885.50	1889.64
Quartz (monocrystalline)	48.0	51.3
Quartz (polycrystalline)	3.2	6.3
Quartz overgrowths	9.6	1.0
Chert	-	-
K-feldspar	-	-
Plagioclase	8.3	11.7
Granitic rock fragments	1.1	0.7
Volcanic rock fragments	5.8	2.2
Metamorphic rock fragments	1.1	0.9
Sedimentary rock fragments	8.5	6.6
Mica	0.3	1.9
Heavy minerals	1.1	-
Organic fragments	-	1.3
Calcite cement	6.6	2.9
Anatase/leucoxene	1.6	-
Authigenic kaolin	4.0	3.4
Detrital clay	-	9.8
Primary porosity	-	-
Secondary porosity	0.8	-
Q (quartz + chert)	71.0	72.6
F (feldspar)	9.7	14.5
R (rock fragments)	19.3	12.9
Mean grain size (mm)	1.06	0.72
Mean grain size (class)	v. coarse	coarse
Sorting (class)	poor	moderate
He-porosity (%) *	10.4	4.9
Permeability (air) (mD) *	0.77	0.05
Grain density (g/cm³) *	2.67	2.65

* soxlet cleaned and humidity dried

FIGURE 1. QFR COMPOSITIONS



Porosity and reservoir quality: Intergranular porosity has been almost completely eliminated by the combined effects of quartz overgrowth and calcite cementation, grain contact dissolution, authigenic clay formation and ductile grain/authigenic clay compaction. Trace primary porosity is preserved where quartz overgrowths are incompletely developed. Nearly all of the small amount (0.8%) of macroporosity is secondary mouldic and intragranular porosity that results from partial dissolution of plagioclase and garnet grains. Secondary pores are widely separated and thus, with nearly all intergranular porosity having been eliminated by the deleterious effects of advanced diagenesis, have no interconnectivity. Accordingly, permeability is very low (0.77mD).

#19 1889.64m

Plates 5-8

Texture and framework grains: Sample is a well compacted, argillaceous, grain/matrix supported, moderately sorted, coarse grained lithic arkose in which framework grains are the same as in the previous sample and also include mica-like chlorite grains and fine organic fragments that locally have well preserved cellular structure. Several closely spaced thin laminae are defined by fine grain size and concentrations of detrital clay and compacted organic fragments.

Clay: Clay is mainly brown detrital clay that is concentrated along laminae, where it is sufficiently abundant to support some framework grains. Authigenic kaolin forms scattered patches and patchy pseudomatrix where labile grains have altered, and authigenic mixed-layer illite/smectite is associated with some altered labile rock fragments.

Diagenesis: Quartz overgrowths locally fill intergranular spaces between juxtaposed quartz grains, but are not as common as in the previous sample due to the presence of abundant clay matrix and pseudomatrix. Within argillaceous laminae, advanced grain contact dissolution and microstylolitisiation were promoted by thinly dispersed, illitic detrital clay matrix, and, elsewhere, grain contact dissolution has produced embayed and sutured grain contacts. Physical compaction effects include ductile deformation of argillaceous rock fragments, mica and organics, locally to form pseudomatrix. Plagioclase is locally replaced by coarsely-crystalline calcite. Secondary porosity is absent in thin-section, but SEM revealed the presence of rare secondary mouldic pores that result from labile grain dissolution.

Porosity and reservoir quality: Intergranular porosity is absent due to the deleterious effects of diagenesis, particularly grain contact dissolution/microstylolitisiation, authigenic kaolin formation, ductile grain/authigenic clay compaction and localised quartz overgrowth cementation. In addition, the rock is cut by several argillaceous laminae, where intergranular spaces are completely filled by detrital clay. Rare secondary mouldic pores do nothing to enhance reservoir quality. With intergranular porosity being absent, permeability is negligible (0.05mD).

4. X-RAY DIFFRACTION ANALYSES

Quantitative XRD analyses are given in Table 2, clay mineralogy is given in Table 3, and annotated XRD traces are presented in Appendix 1.

Quantitative XRD analyses complement the thin-section analyses but cannot be compared directly. This is because thin-section clay includes microporosity, and therefore total thin-section clay is elevated relative to other components. In addition, thin-section detrital clay and rock fragment components include quartz, plagioclase, mica/illite, mixed-layer illite/smectite, kaolin and chlorite that are recorded as these phases by XRD.

Quantitative XRD analyses show that the two sandstones contain similar amounts of quartz (74.2% mean), plagioclase (8.4%), kaolin (4.2% mean), chlorite (1.8% mean) and illite/mica (1.7% mean), but differing amounts of mixed-layer illite/smectite (3.3%, 8.5%) and calcite (6.8%, 1.0%).

Fine-fraction XRD analyses (Table 3) indicate that kaolin dominates over illite/mica, mixed-layer illite/smectite and chlorite. Mixed-layer illite/smectite is an ordered variety containing 60-65% illite interlayers. Highly smectitic clays are absent.

Detected kaolin occurs as a labile grain alteration product and may also be a constituent of detrital clay matrix and some argillaceous sedimentary rock fragments. Detected illite occurs as fine detrital mica and also as a constituent of detrital clay matrix, argillaceous sedimentary rock fragments and sericitised plagioclase. Detected mixed-layer illite/smectite appears to be a major constituent of detrital clay matrix, being far more abundant in argillaceous #19 than in non-argillaceous #7, and also occurs as a labile grain alteration product. Detected chlorite is detrital, occurring as an original constituent of metasedimentary rock fragments and altered volcanic rock fragments.

TABLE 2. BULK-ROCK XRD ANALYSES (weight %)

Sample #	Depth (m)	Qtz	PF	Ka	I/M	I/S	Chl	Ca
7	1885.50	74.5	9.0	4.0	1.0	3.3	1.4	6.8
19	1889.64	73.8	7.8	4.4	2.3	8.5	2.2	1.0

Qtz = quartz; PF = plagioclase; Ka = kaolin; I/M = illite/mica; I/S = mixed-layer illite/smectite; Chl = chlorite; Ca = calcite

TABLE 3. FINE-FRACTION CLAY MINERALOGY

Sample #	Depth (m)	Ka	I/M	I/S	Sm	Chl
7	1885.50	M	m	m	-	m
19	1889.64	M	T	m	-	m

Ka = kaolin; I/M = illite/mica; I/S = illitic mixed-layer illite/smectite (60-65% illite interlayers); Sm = smectite; Chl = chlorite

A = abundant; M = major; m = minor; T = trace

5. SUMMARY AND CONCLUSIONS

- Samples from 1885.50m and 1889.64m in Megascolides-1ST are a poorly sorted, very coarse grained feldspathic litharenite and an argillaceous, moderately sorted, coarse grained lithic arkose, respectively.
- Framework grains are mainly quartz, plagioclase and a variety of rock fragments that are indicative of a polymictic continental provenance dominated by garnetiferous granodiorites and which also included siliciclastic sedimentary rocks, low-grade metasedimentary rocks and intermediate volcanic rocks.
- Detrital clay is concentrated along thin laminae at 1889.64m. Authigenic kaolin forms scattered patches and patchy pseudomatrix where labile grains, particularly plagioclase, have altered. Authigenic clay also includes mixed-layer illite/smectite that is associated with some altered labile rock fragments.
- Clay minerals detected by XRD are kaolin and subordinate illite/mica, mixed-layer illite/smectite (60-65% illite interlayers) and chlorite.
- Other diagenetic effects besides authigenic clay formation include quartz overgrowth and calcite cementation, physical compaction, grain contact dissolution/microstylolitis and feldspar/garnet dissolution. Where quartz overgrowth cementation was not inhibited by clay, compacted grains and earlier-formed calcite cement, quartz overgrowths completely fill intergranular spaces to form triple point grain contacts.
- Samples contain little or no primary intergranular porosity due to the deleterious effects of advanced diagenesis. Porosity reduction at 1889.64m also results from detrital clay pore filling along argillaceous laminae. Secondary labile grain dissolution pores, being few and far between, do nothing to enhance reservoir quality.
- With virtually all intergranular spaces being filled by cement, clay and compacted ductile grains, effective porosity is absent and permeabilities are consequently very low (0.77mD, 0.05mD).

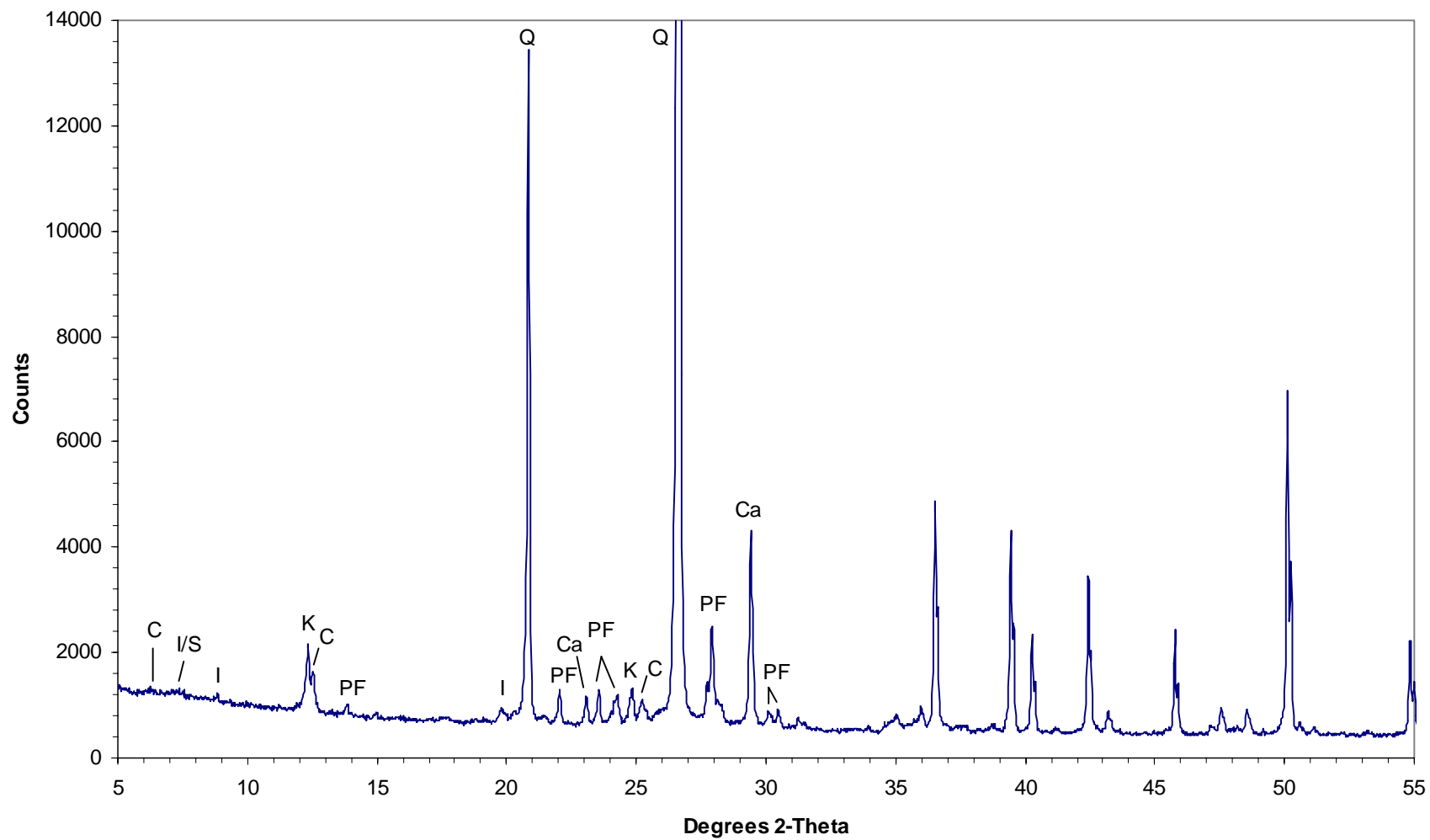
APPENDIX 1

X-RAY DIFFRACTION TRACES

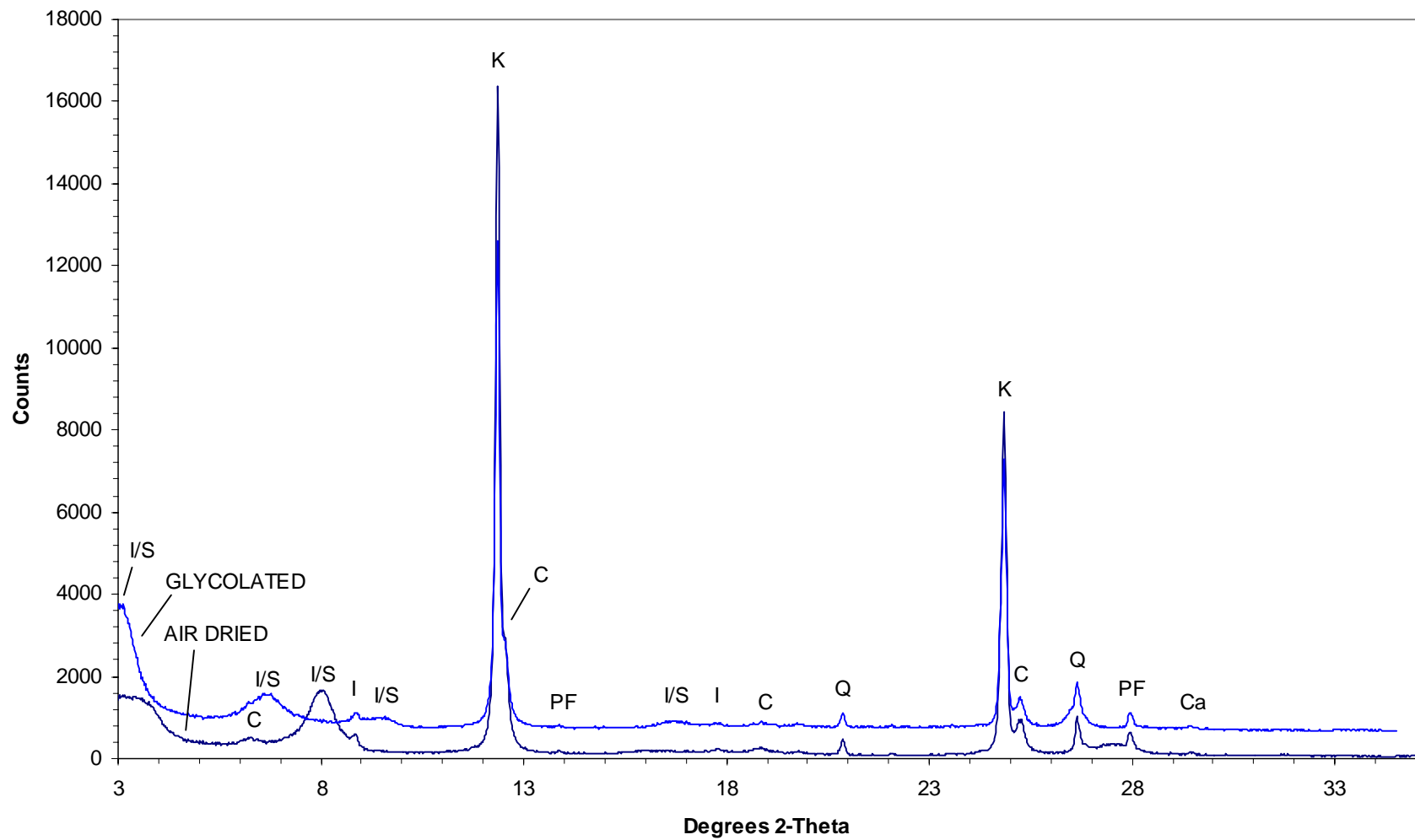
Key to abbreviations:

C	=	chlorite
Ca	=	calcite
I	=	illite/mica
I/S	=	mixed-layer illite/smectite
K	=	kaolin
PF	=	plagioclase
Q	=	quartz

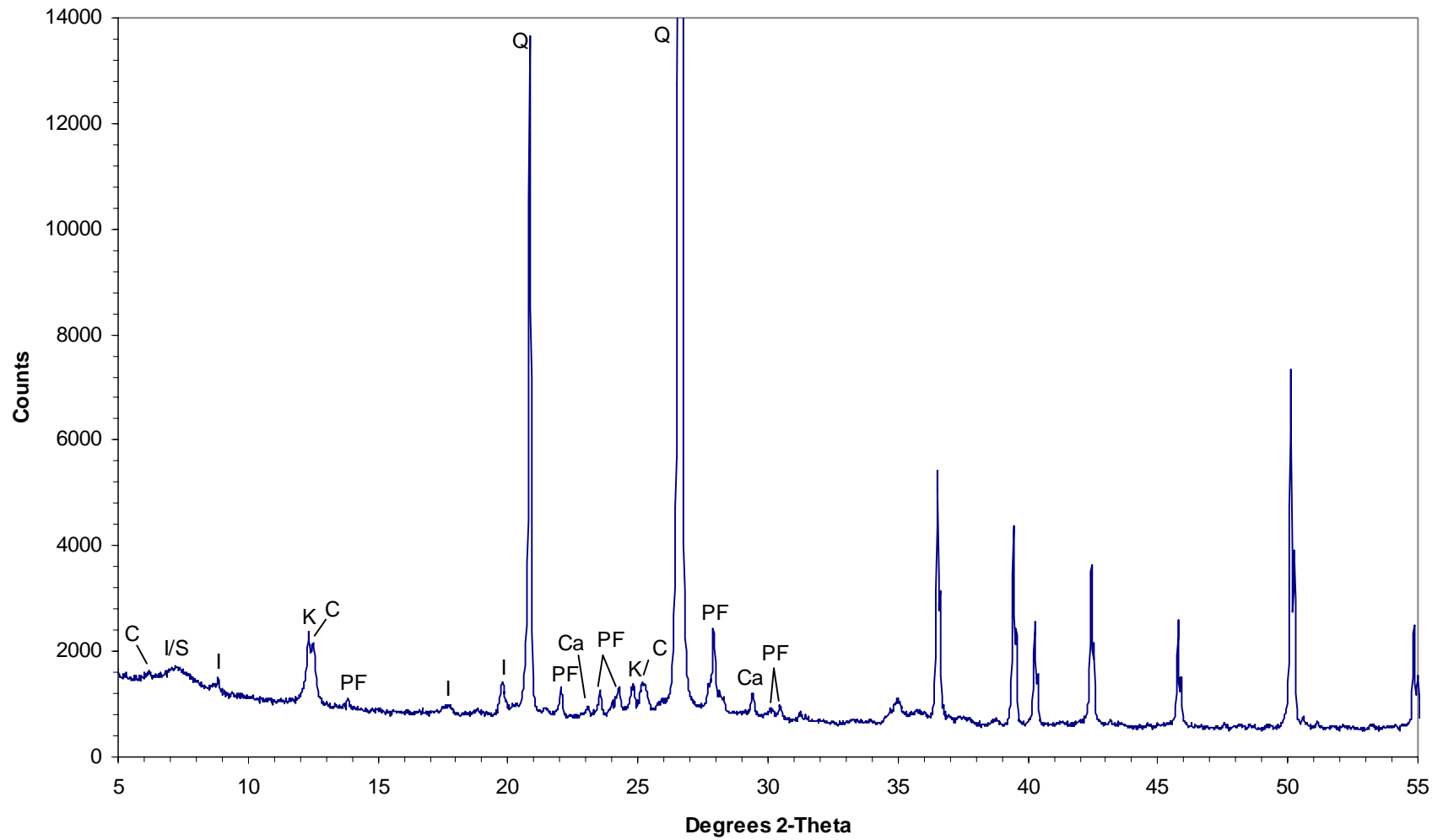
#7 1885.50m
Bulk rock



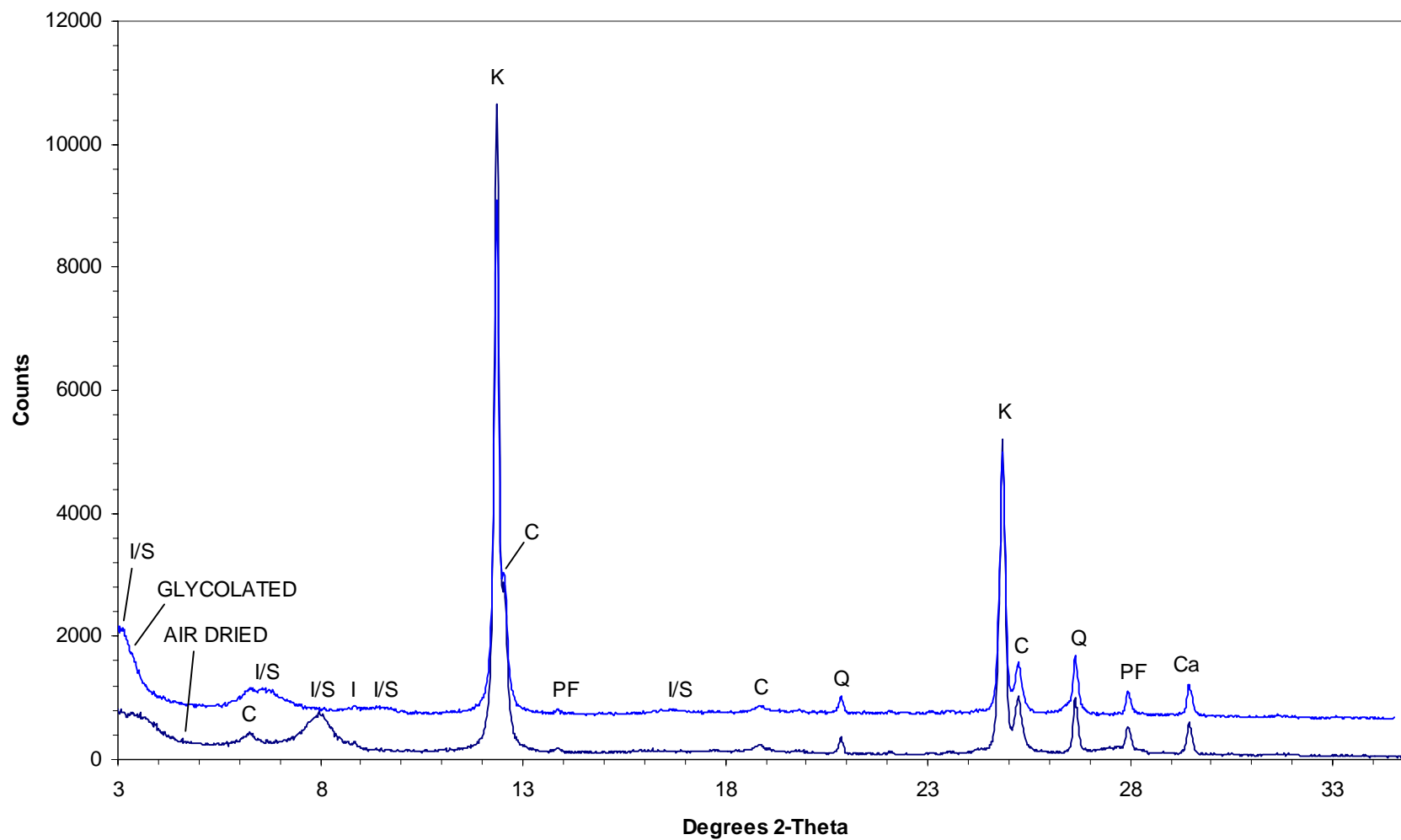
#7 1885.50m
Fine fraction



#19 1889.64m
Bulk rock



#19 1889.64m
Fine fraction



APPENDIX 2

MICROGRAPHS

KEY TO PLATES IN APPENDIX 2

Sample #	Depth (m)	Plate #
7	1885.50	1, 2, 3*, 4*
19	1889.64	5, 6, 7*, 8*

* SEM micrographs

PLATE 1 #7 1885.50m

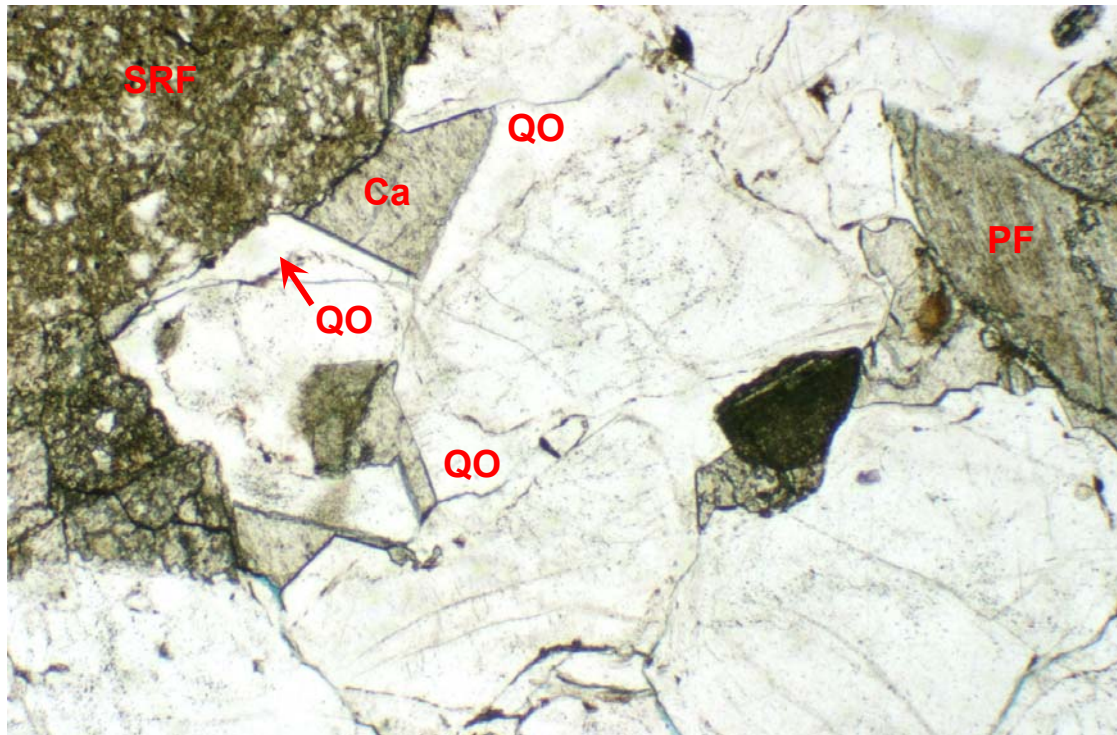
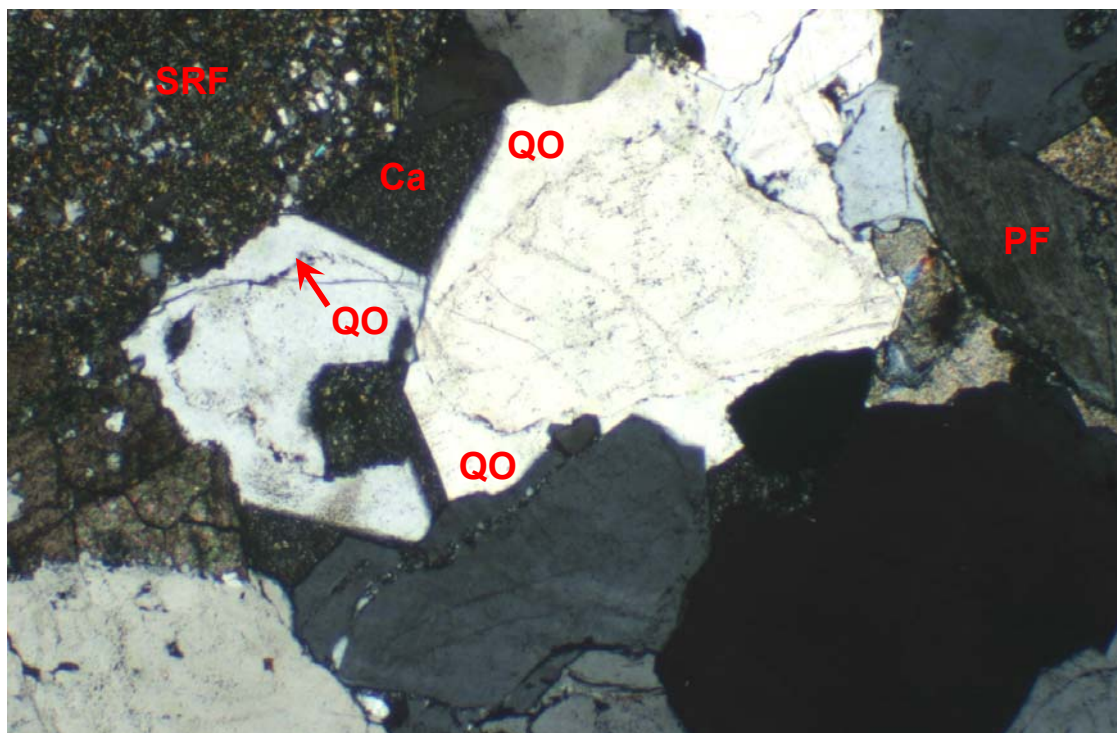


FIGURE 1 Plane polarised light
FIGURE 2 Crossed polarisers

0.4 mm



Very coarse grained feldspathic litharenite in which all intergranular spaces between quartz and granitic plagioclase (PF) grains and a pebble-sized sedimentary rock fragment (indurated silty mudrock) (SRF) are tightly filled by quartz overgrowth (QO) and calcite (Ca) cement. Detail is shown in Plate 2. $K = 0.77\text{mD}$ (Thin-section micrographs)

PLATE 2 #7 1885.50m (cont.)

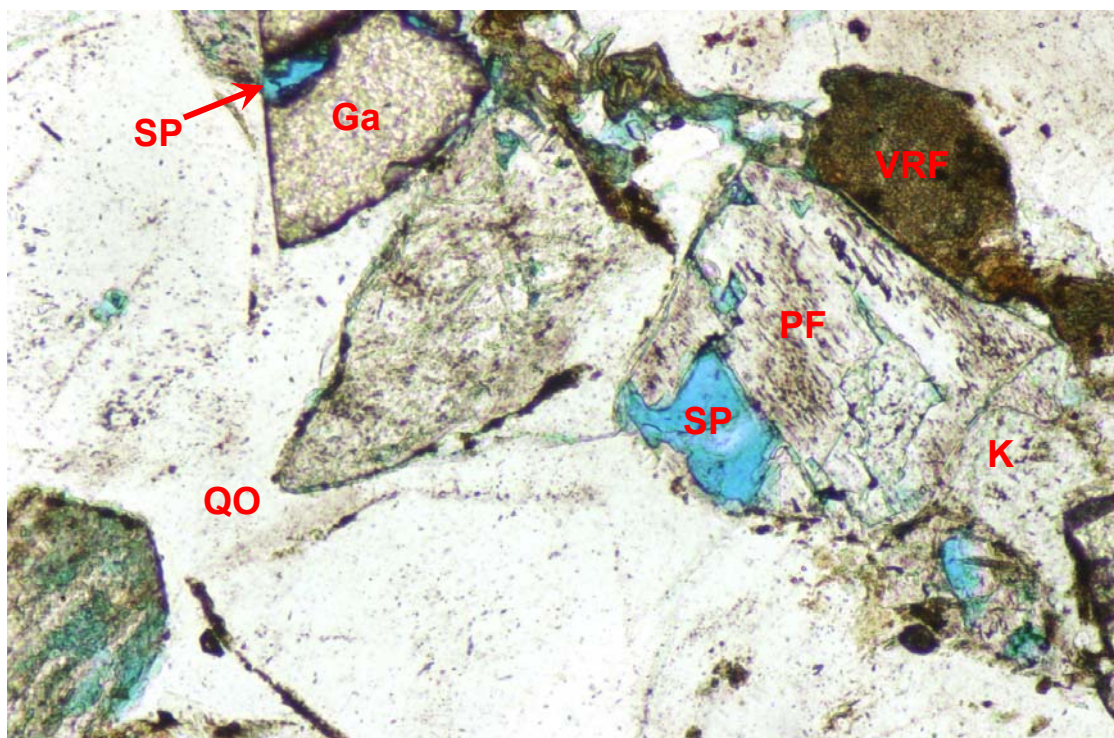
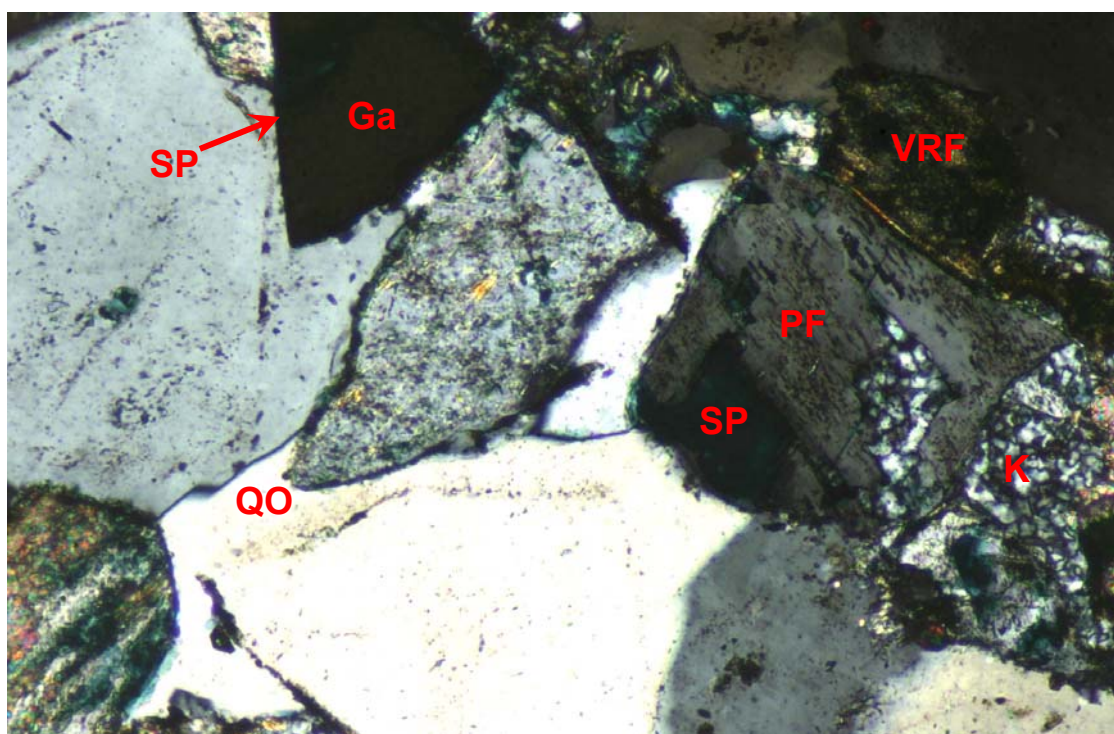


FIGURE 1 Plane polarised light
FIGURE 2 Crossed polarisers

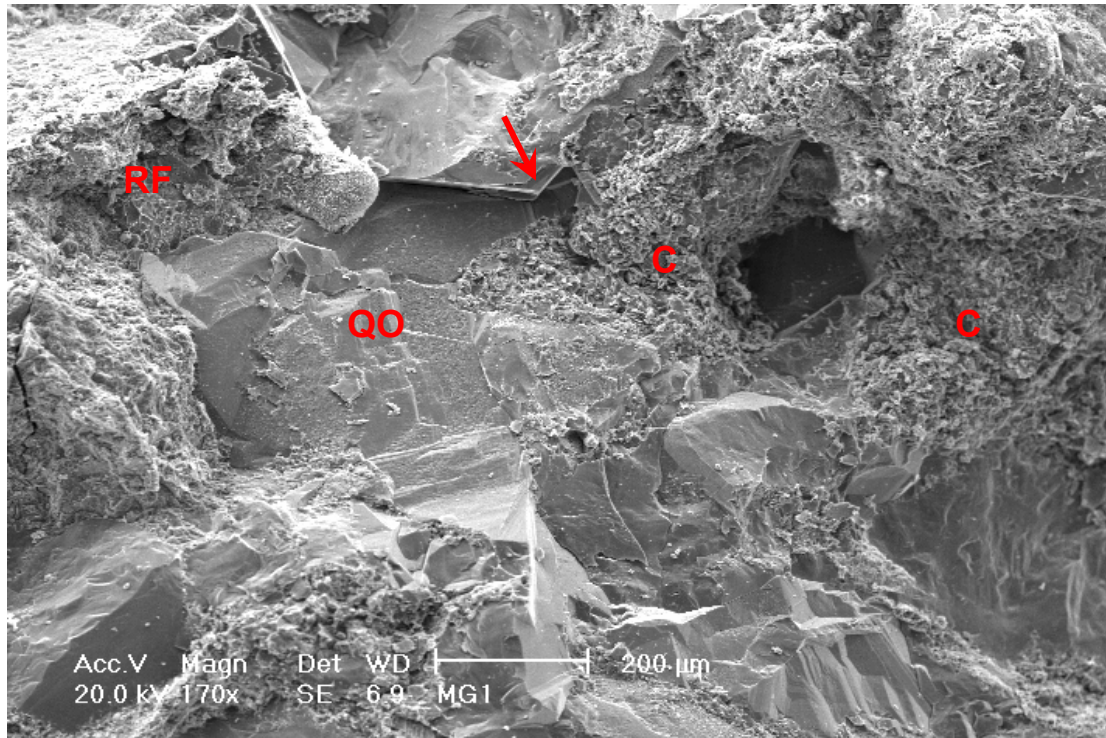
0.2 mm



Isolated secondary pores (SP) result from partial dissolution of plagioclase (PF) and accessory garnet (Ga) grains. With intergranular spaces being tightly filled by quartz overgrowth cement (QO), the pores have no interconnectivity. Authigenic kaolin (K) is a product of plagioclase alteration. An altered volcanic rock fragment (VRF) is also marked. $K = 0.77\text{mD}$ (Thin-section micrographs)

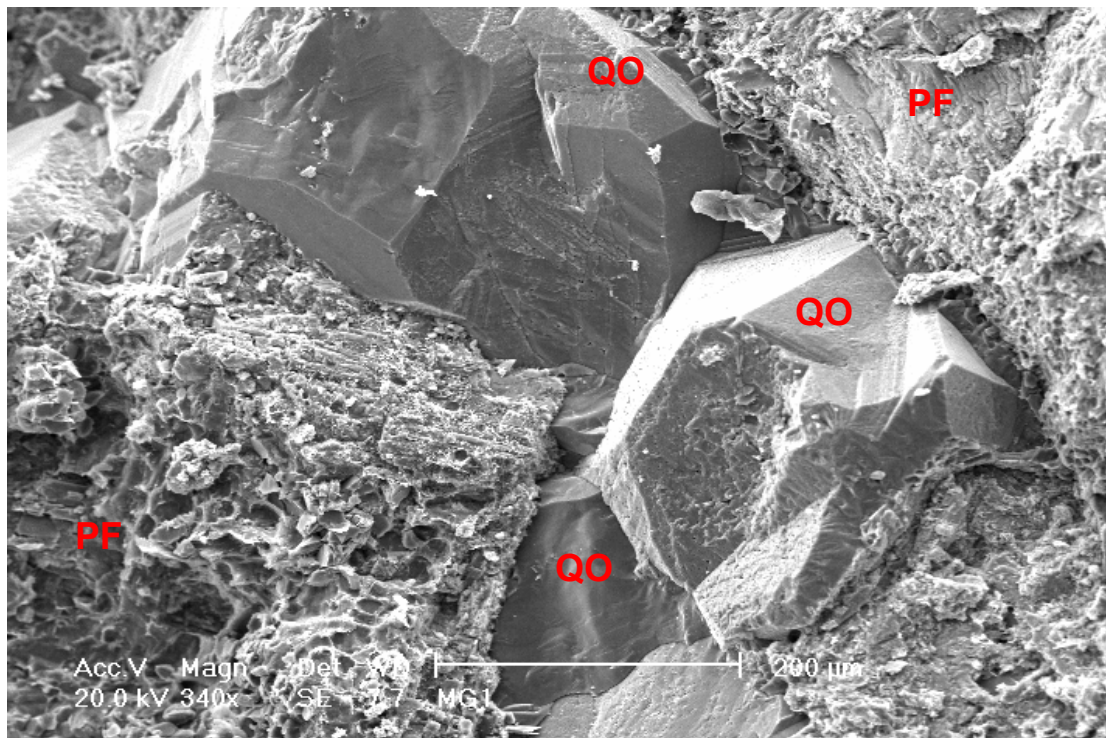
PLATE 3 #7 1885.50m (cont.)

FIGURE 1



Tight sandstone in which quartz overgrowths (QO) completely fill intergranular spaces to form triple point grain contacts (arrow). Intergranular spaces are also filled by compacted argillaceous rock fragments (RF) and authigenic clay (C). (SEM micrograph)

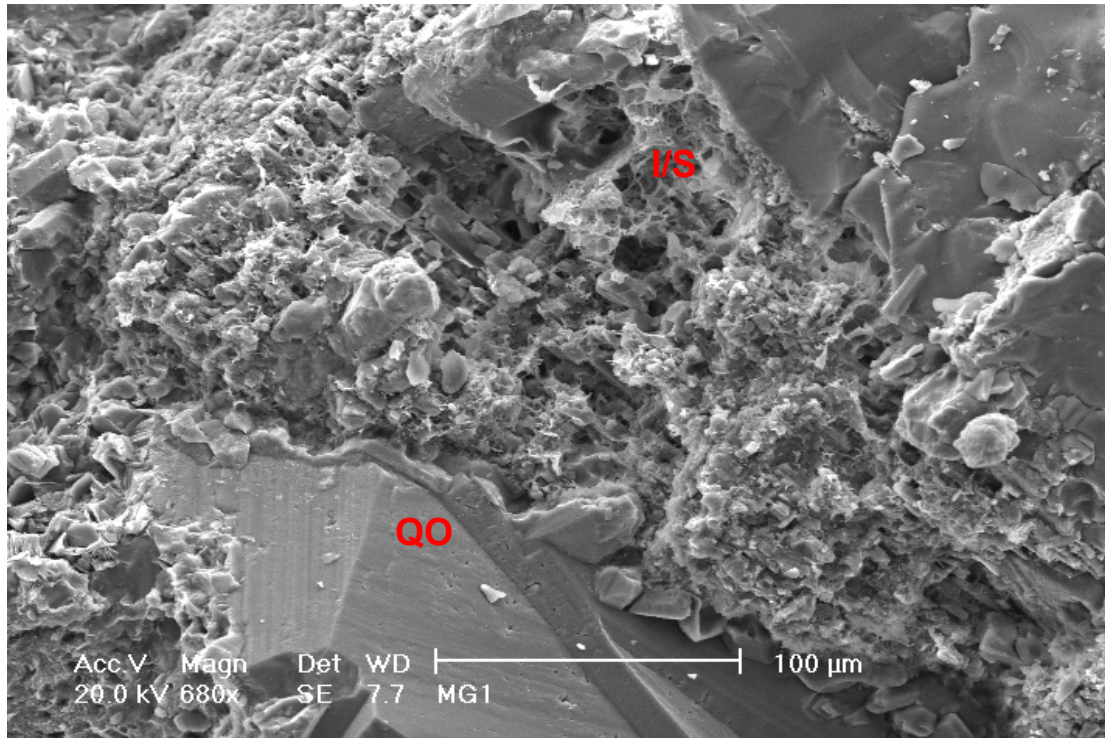
FIGURE 2



Intergranular spaces between quartz and altered plagioclase (PF) grains are tightly filled by quartz overgrowth cement (QO). (SEM micrograph)

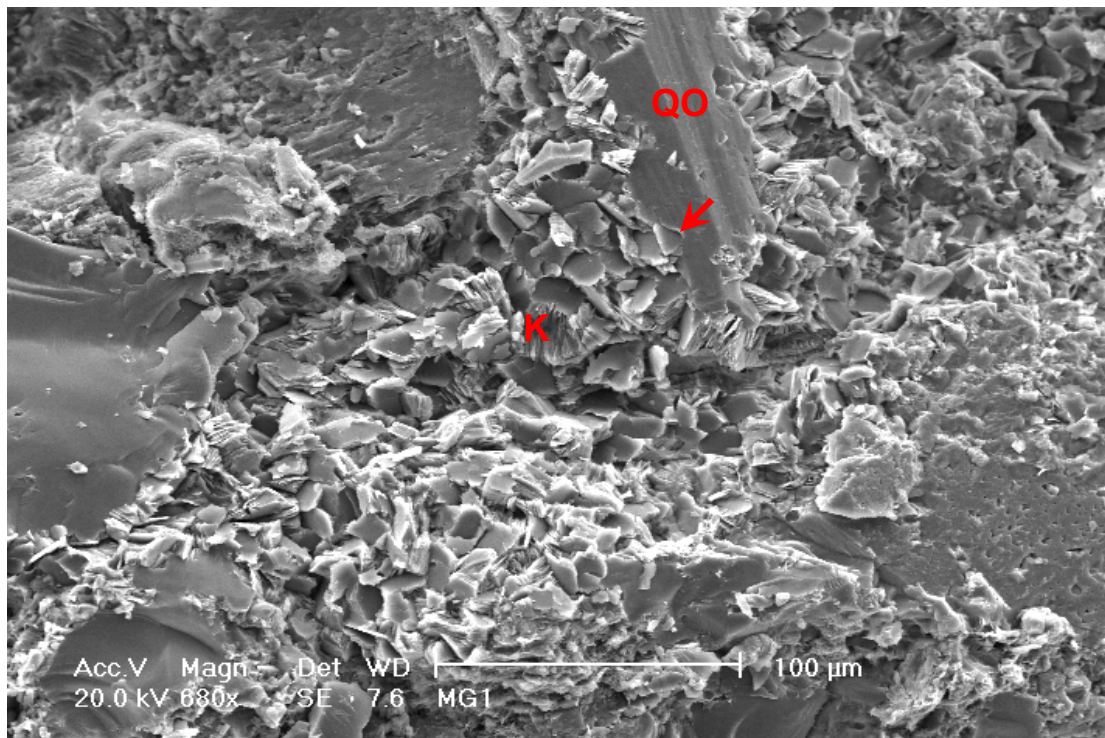
PLATE 4 #7 1885.50m (cont.)

FIGURE 1



Clay includes authigenic mixed-layer illite/smectite (I/S) that results from labile grain decomposition. Intergranular pores are filled by quartz overgrowths (QO). (SEM micrograph)

FIGURE 2



Authigenic kaolin (K) occurs as a breakdown product of plagioclase. Quartz overgrowths (QO) enclose (arrow) and thus postdate authigenic kaolin. (SEM micrograph)

PLATE 5 #19 1889.64m

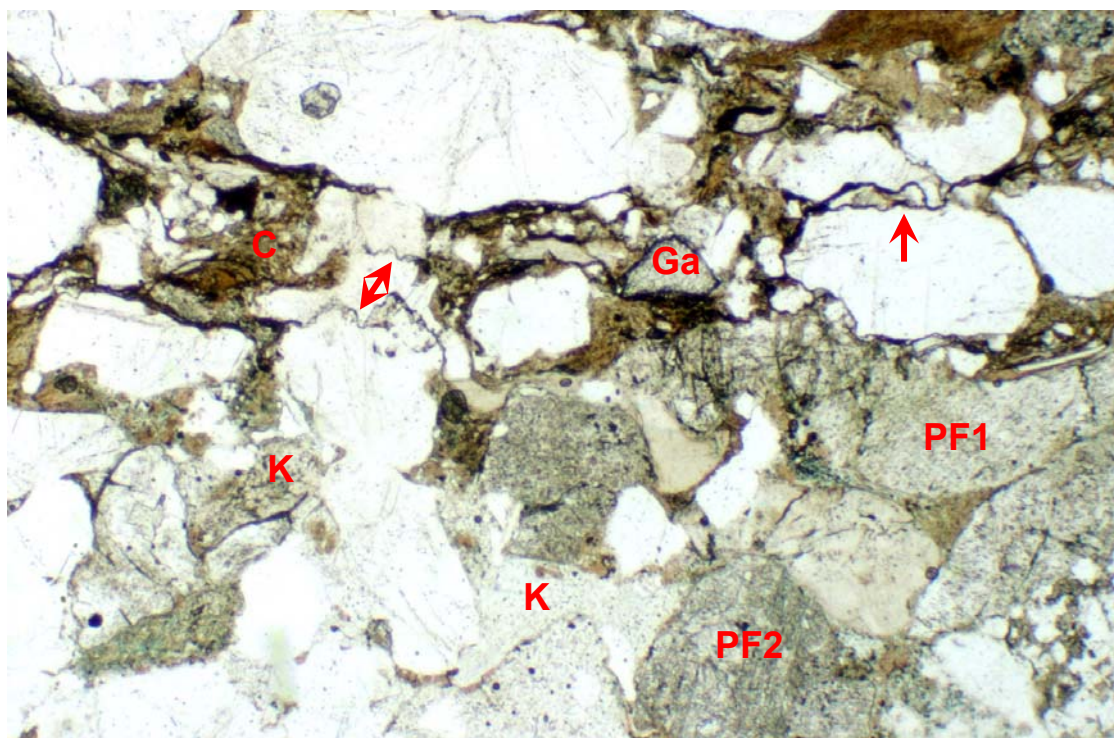
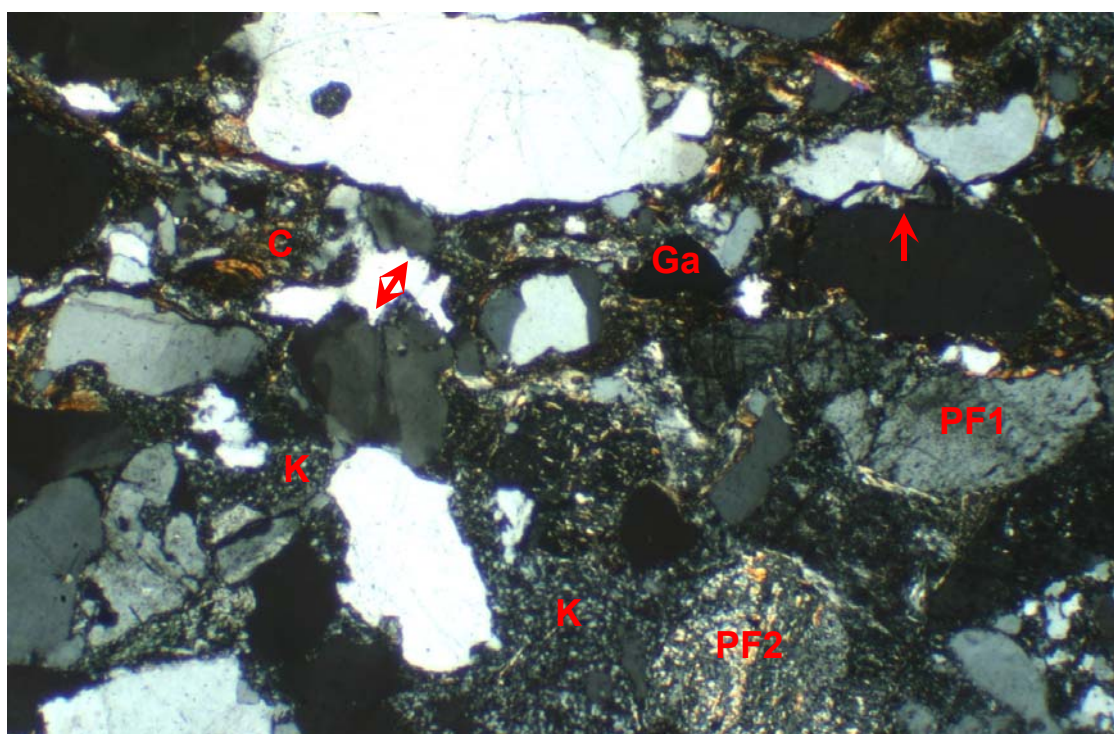


FIGURE 1 Plane polarised light
FIGURE 2 Crossed polarisers

0.4 mm



In this coarse grained lithic arkose, detrital clay (C) is concentrated along a thin, argillaceous lamination (top half of micrographs), where it has promoted microstylolitis between quartz grains (arrows). Elsewhere, intergranular spaces are filled by authigenic kaolin (K) and compacted ductile grains. Framework grains include fresh untwinned plagioclase (PF1), sericitised plagioclase (PF2) and accessory garnet (Ga). $K = 0.05\text{mD}$ (Thin-section micrographs)

PLATE 6 #19 1889.64m (cont.)

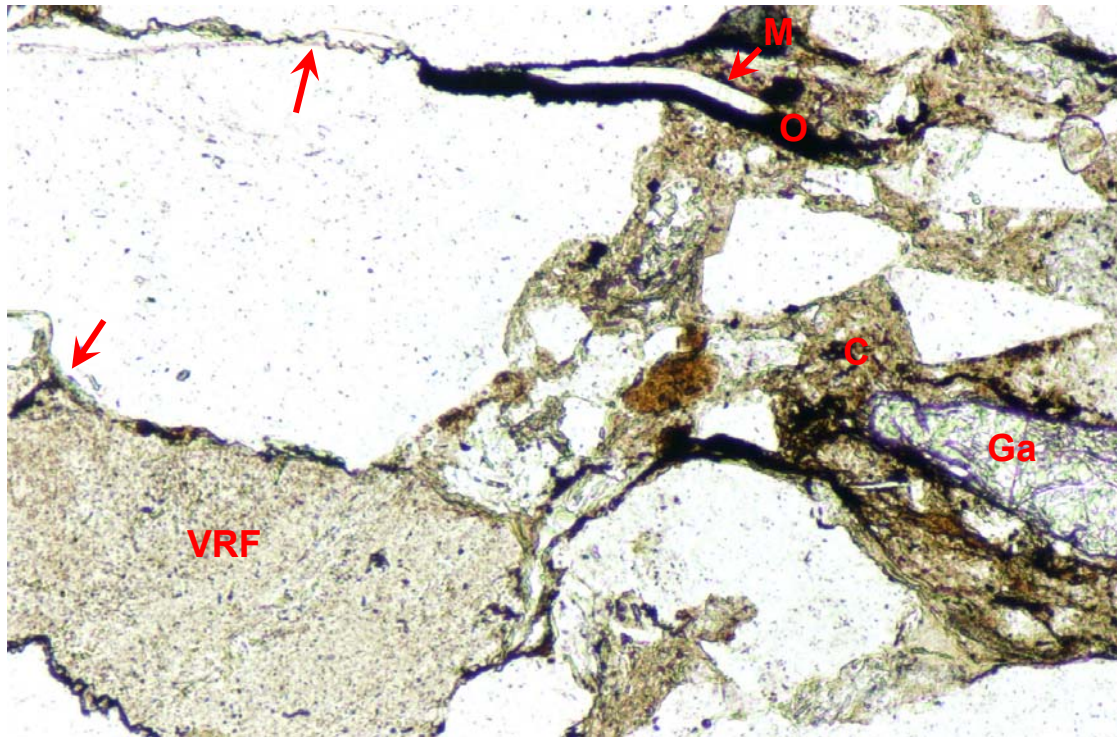
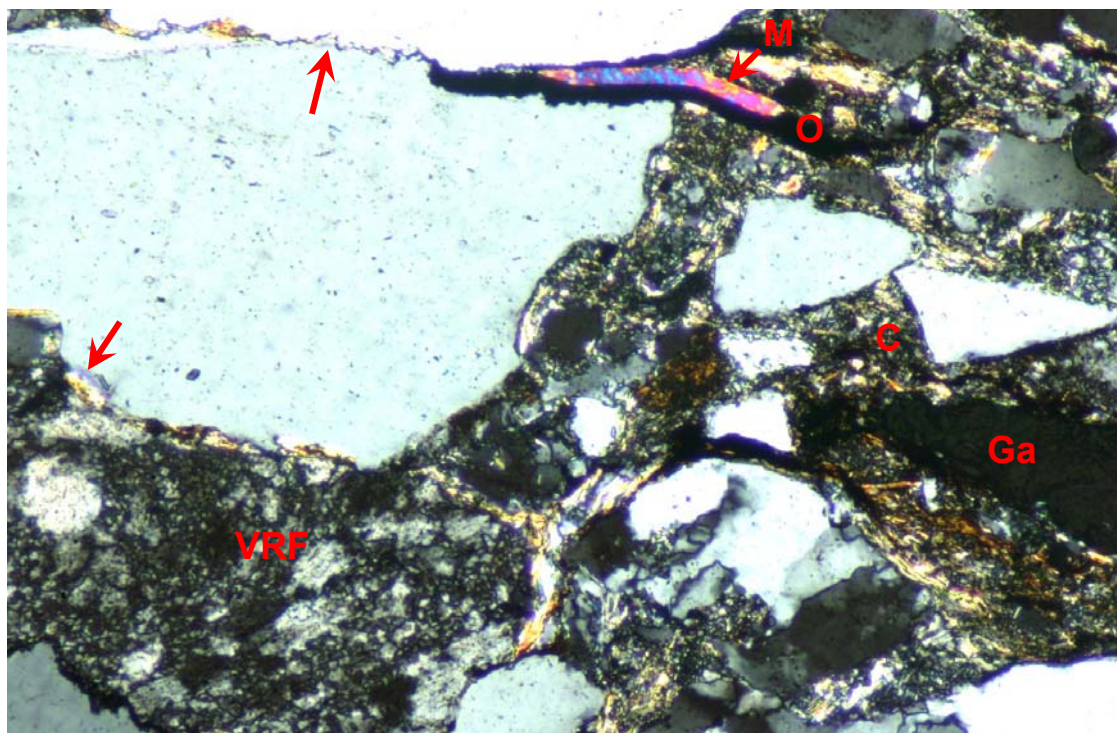


FIGURE 1 Plane polarised light
FIGURE 2 Crossed polarisers

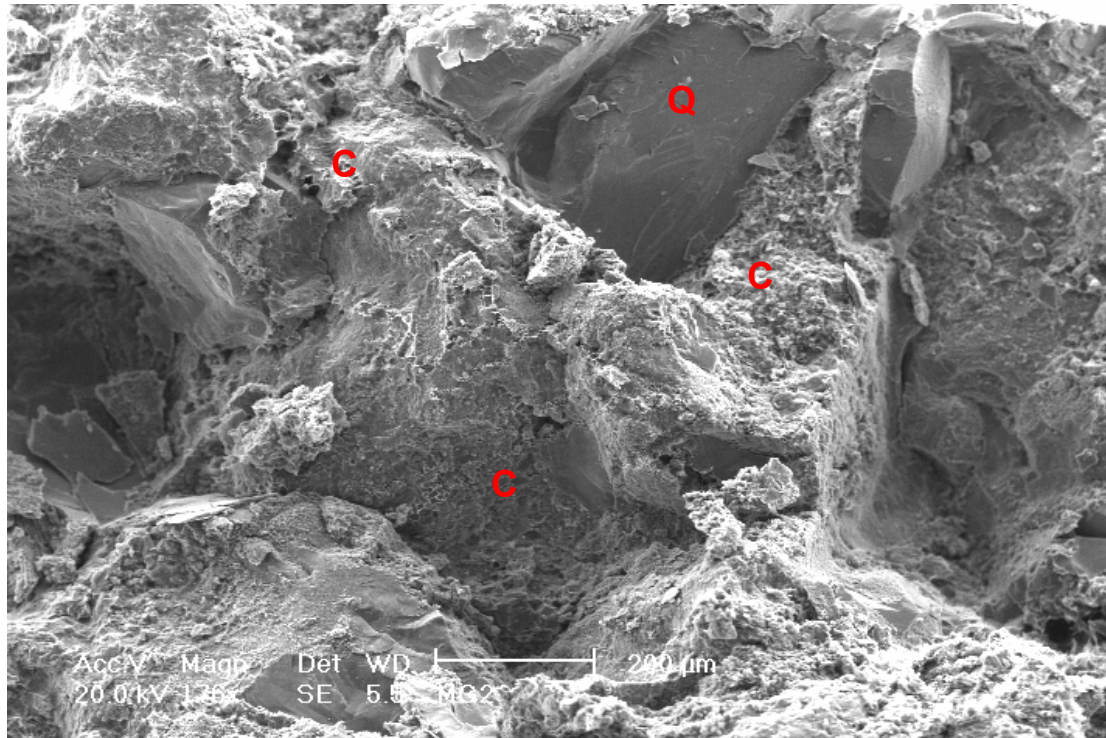
0.2 mm



In this area, intergranular spaces are filled by detrital clay matrix (C) and there has also been porosity destruction by the formation of microstylolitic grain contacts (arrows) between quartz grains and a silicified volcanic rock fragment (VRF). Detrital grains also include mica (M), organics (O) and accessory garnet (Ga). $K = 0.05\text{mD}$ (Thin-section micrographs)

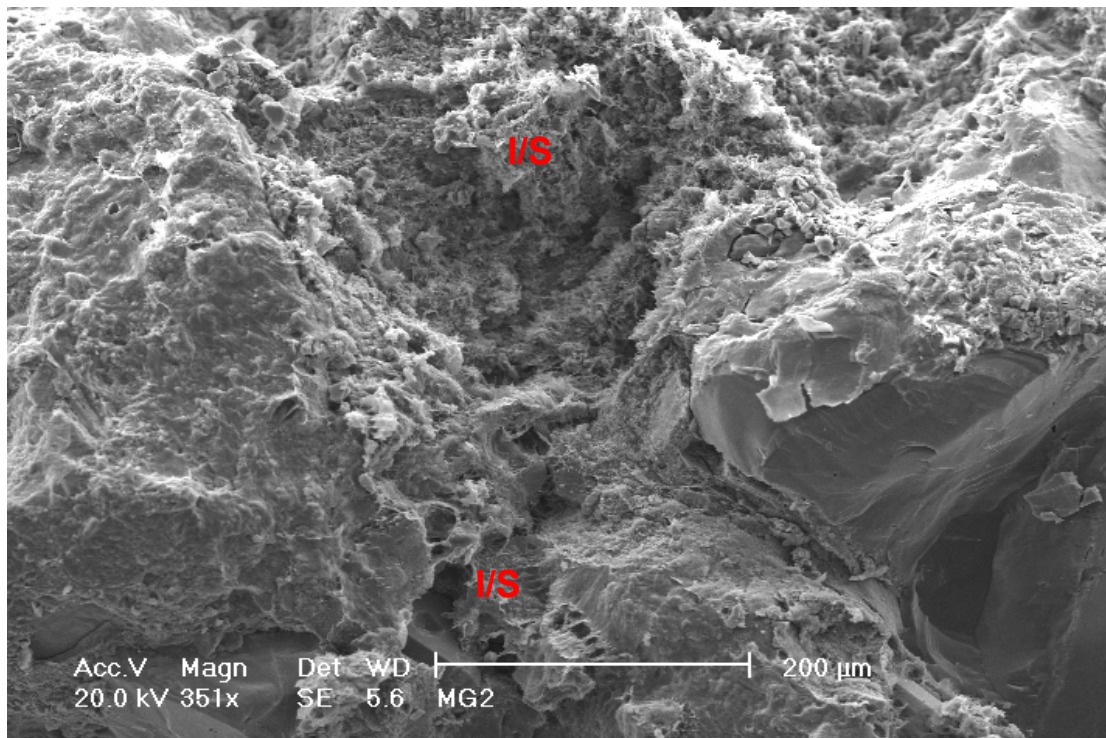
PLATE 7 #19 1889.64m (cont.)

FIGURE 1



Tight sandstone in which intergranular spaces between quartz grains (Q) are completely filled by compacted ductile grains and clay (C), the presence of which has prevented quartz overgrowth cementation in field of view. (SEM micrograph)

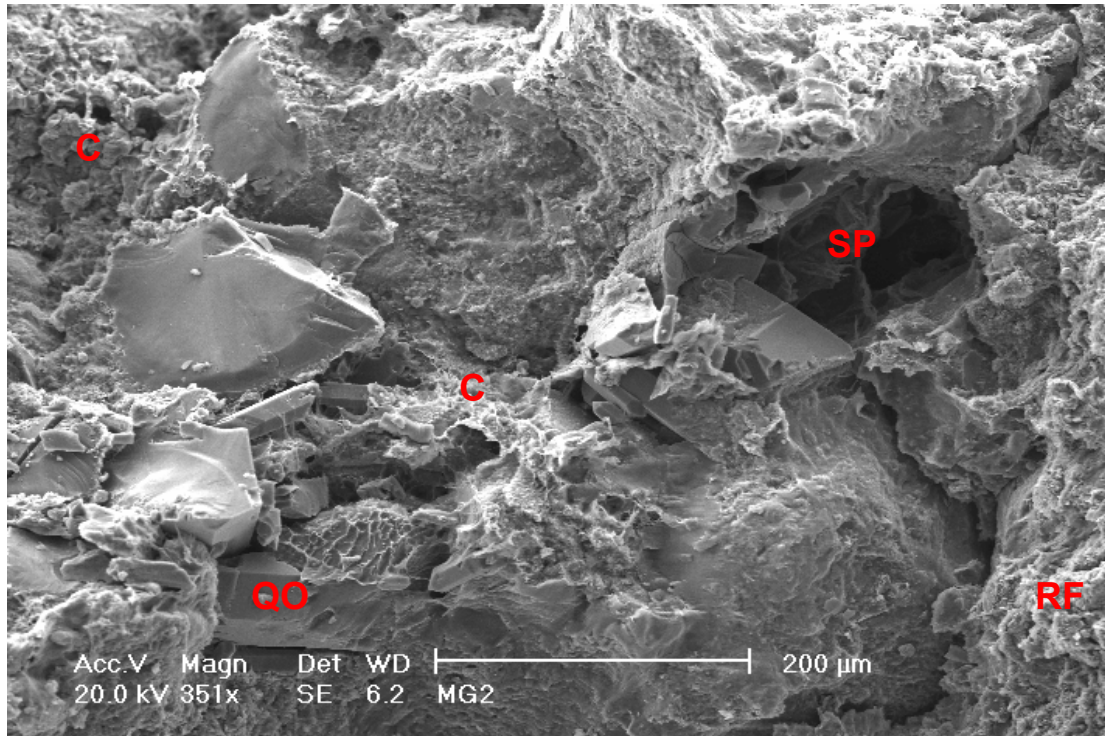
FIGURE 2



Authigenic mixed-layer illite/smectite pseudomatrix (I/S) is a product of argillaceous rock fragment compaction and alteration. (SEM micrograph)

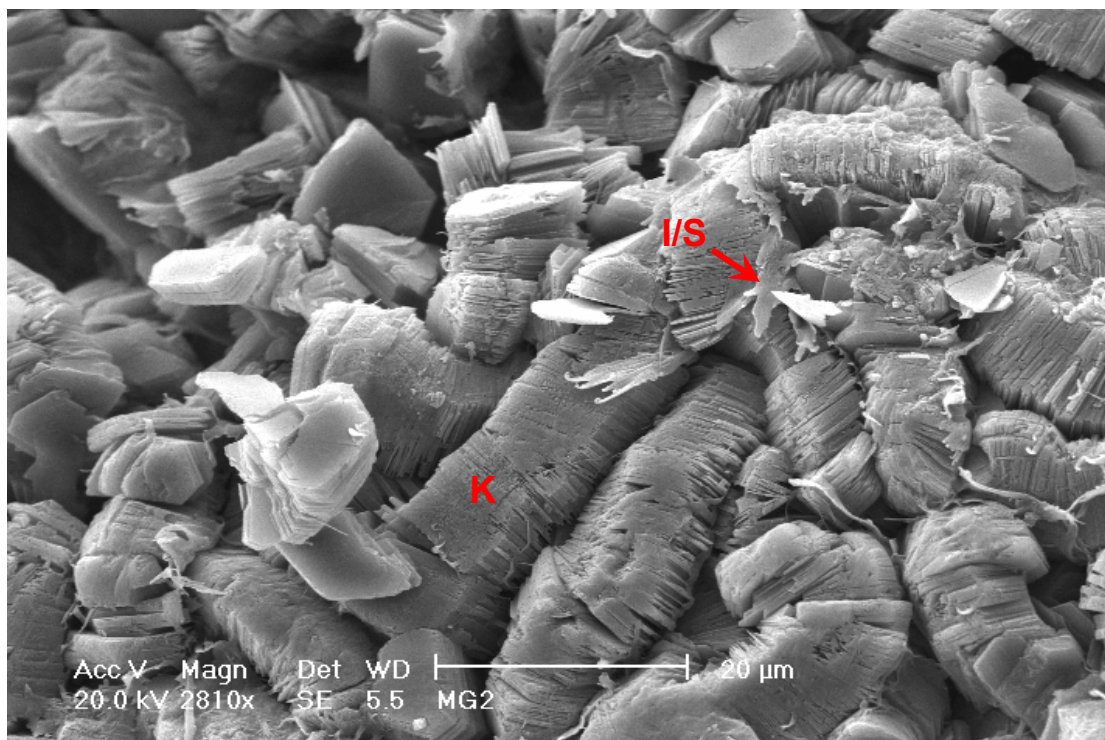
PLATE 8 #19 1889.64m (cont.)

FIGURE 1



A rare secondary mouldic labile grain dissolution pore (SP) is surrounded by sandstone in which intergranular spaces are completely filled by quartz overgrowths (QO), clay (C) and compacted rock fragments (RF). (SEM micrograph)

FIGURE 2



Detail of typical authigenic kaolin (K) that results from plagioclase alteration. Minor authigenic mixed-layer illite/smectite (I/S) is associated with the kaolin. (SEM micrograph)